Micro-mechanically guided high-throughput alloy design exploration towards metastability-induced H embrittlement resistance

PI: C. Cem Taşan, Ju Li, Bilge Yildiz (MIT),
Joost J. Vlassak (Harvard)

DOE project Award No.: DE-EE0008830

June 7th, 2023

Massachusetts Institute of Technology

Project Goal

- Develop a novel high-throughput compositional and microstructures screening approach to develop new alloys with superior hydrogen embrittlement (HE)-resistance, by specifically focusing on utilization of metastability effects on toughening. This includes:

  (i) Technique development of high-throughput screening (HTS) for HE-resistance (***Methods***)

  (ii) Discovery of new metallic materials with superior HE-resistance (***Materials***)

  (iii) Multiscale verification of HE-resistance of the new alloys (***Mechanisms***)

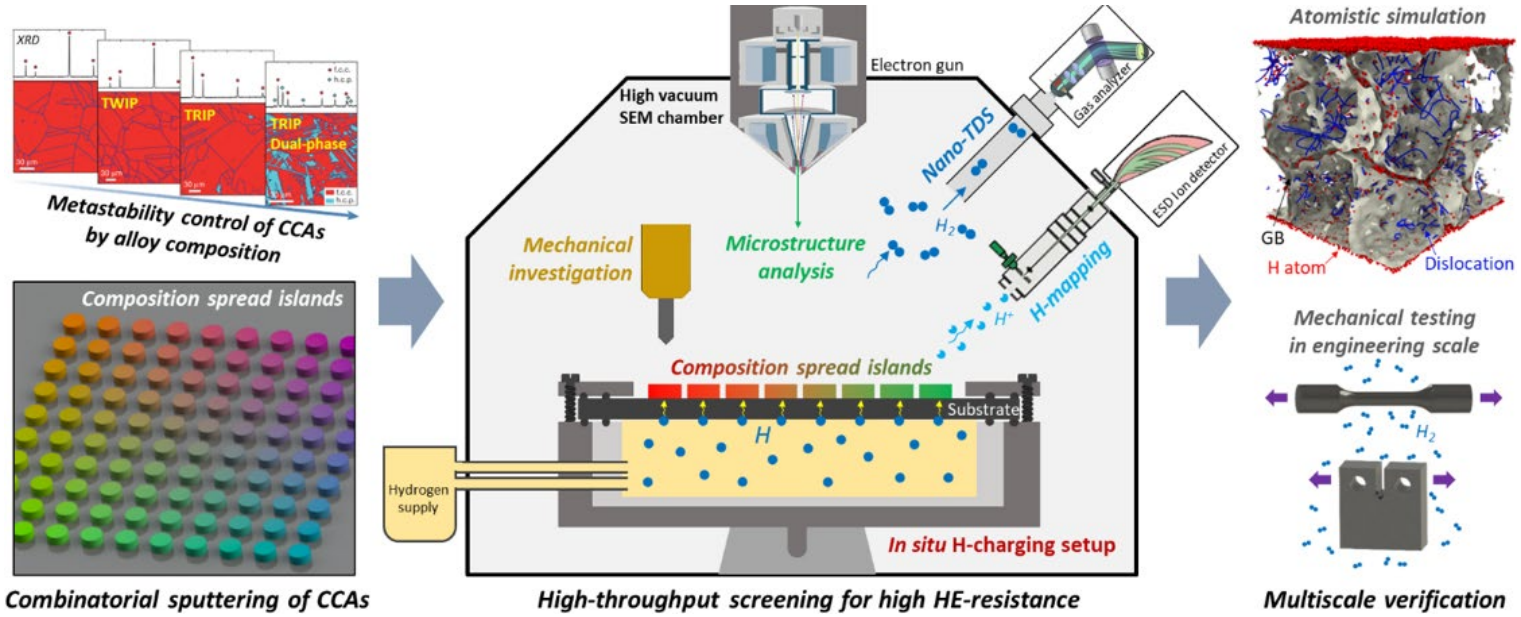

Overview

Timeline

- Project Start Date: 04/01/20
- Project End Date: 05/31/23

Barriers

- Key barriers addressed in the project are:
  - Hydrogen delivery, E. Gaseous Hydrogen Storage and Tube Trailer Delivery Costs
  - Hydrogen storage, G. Materials of construction

Budget

- Total Project Budget: $1,250,000
- Total DOE Share: $1,000,000
- Total Cost Share: $250,000
- Total DOE Funds Spent*: $990,195.31
- Total Cost Share Funds Spent*: $250,000.00

*Estimated as of 03/31/23

Partners

- Project lead: C. Cem Tasan (MIT)
- Co-PIs: Ju Li, Bilge Yildiz (MIT), Joost J. Vlassak (Harvard)
- Partner organization: ATI

Relevance and Potential Impact

Methods: The outcome can significantly accelerate new metallic material exploration process and screening of HE-resistance, which are required for “Safe, Lower Cost Containment Technologies” in HFTO MYRDD.

Materials/Mechanisms: Explore complex-concentrated alloy (CCA) space in which phase metastability (related to deformation-induced phase transformation and mechanical twinning) can be utilized to enhance HE-resistance.

Barrier from HFTO MYRDD	**Impact from this project**
Hydrogen delivery, E. Gaseous Hydrogen Storage and Tube Trailer Delivery Costs	Provide novel methods to drastically reduce the required R&D period for new alloy development as well as H-related physical property screening of multiple alloys
Hydrogen storage, G. Materials of construction	

Approach: *Integrated high-throughput alloy design strategy*

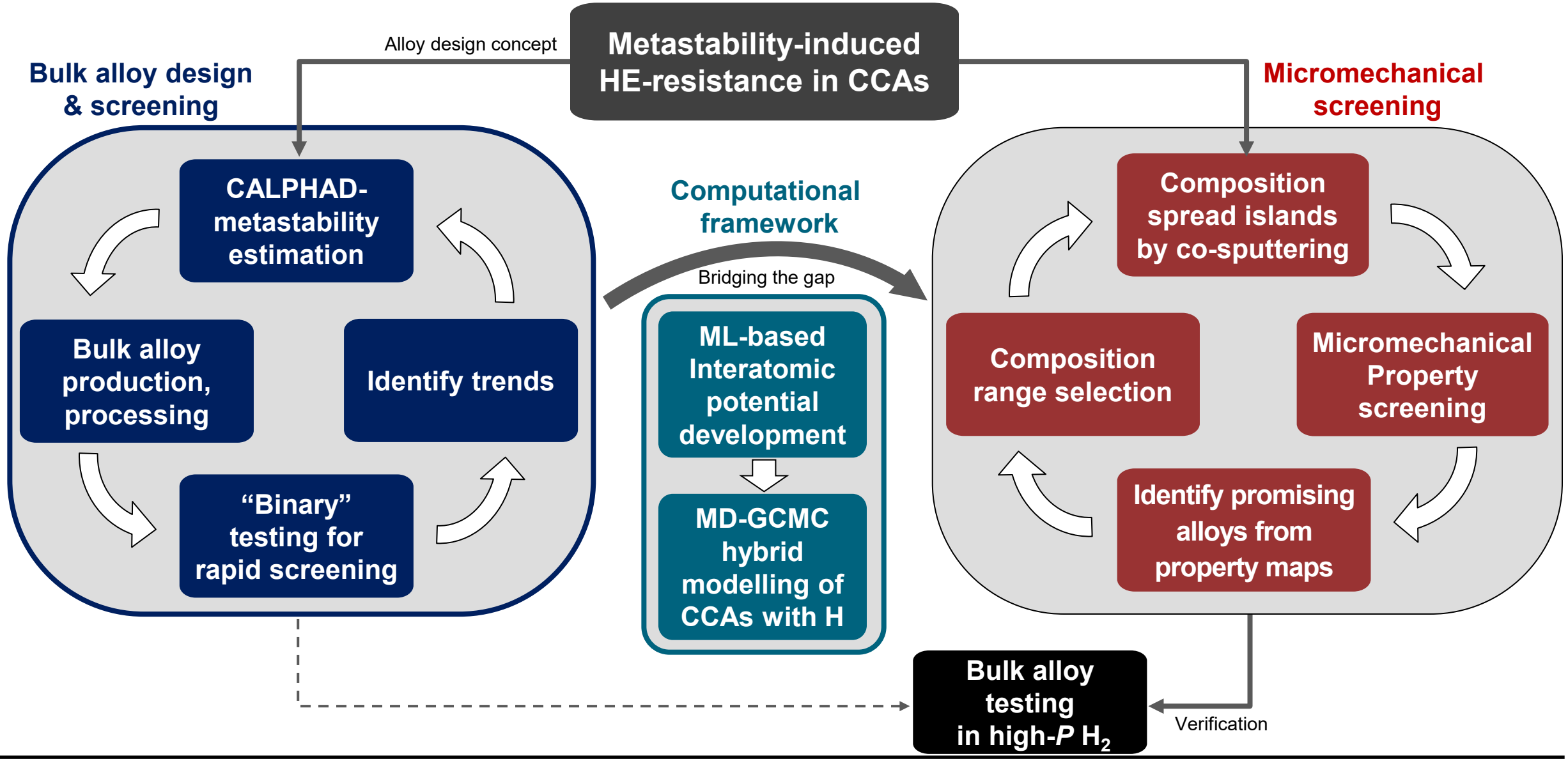

Approach: *Integrated high-throughput alloy design strategy*

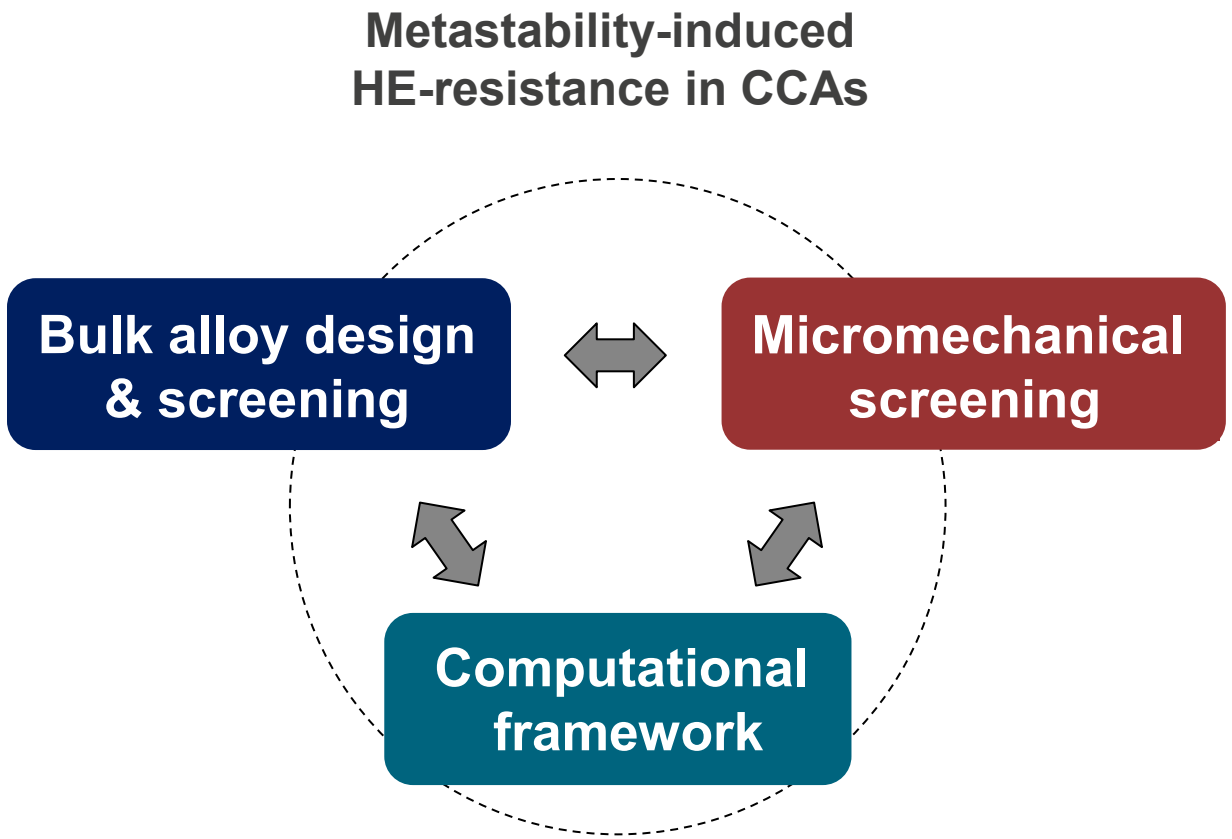

Brief Summary of Past Results

Bulk alloy design & screening

CALPHAD: Austenite stability estimation

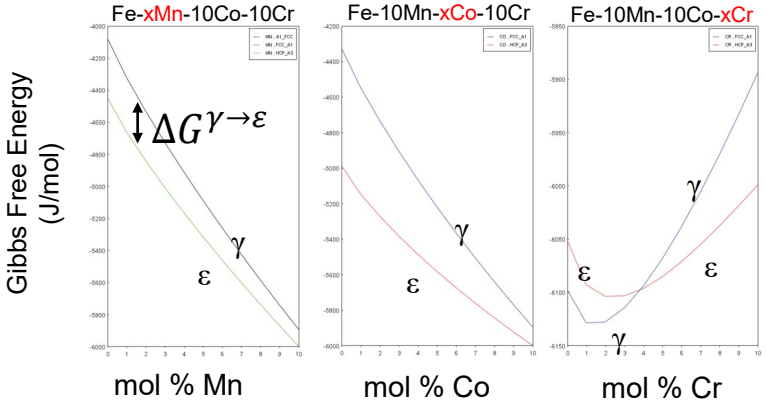

Alloy selection and production

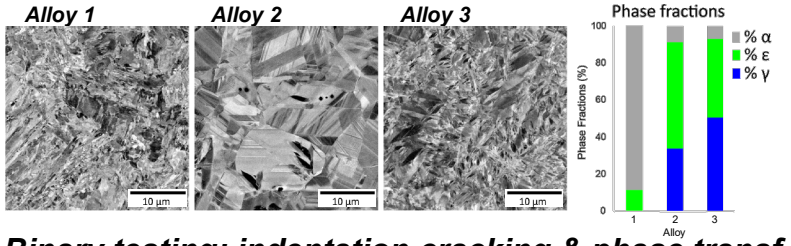

Binary testing: indentation cracking & phase transf.

	Pre-H Indentation		Post-H Indentation		Post-Outgassing Indent.	
Alloy	α' transf?	Cracking?	α' transf?	Cracking?	α' transf?	Cracking?
2	Y	N	Y	N	Y	N
3	Y	N	N	Y	N	Y

Micromechanical screening

Deposition on 8´´ wafer

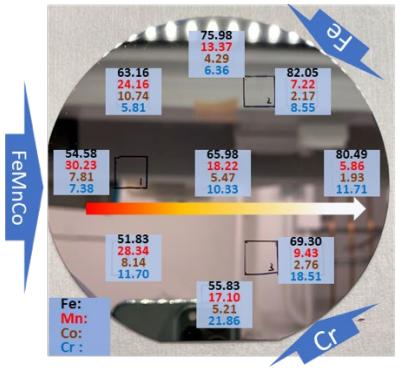

Indentation spots

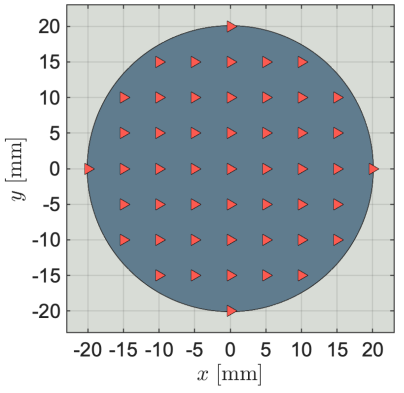

Before charging

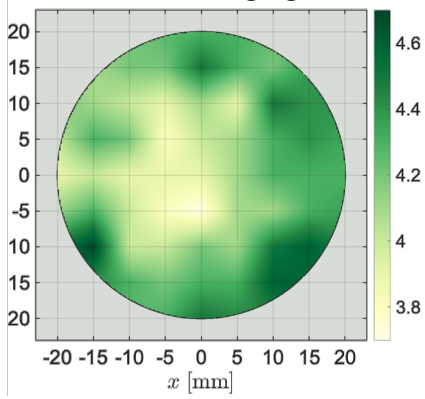

After charging

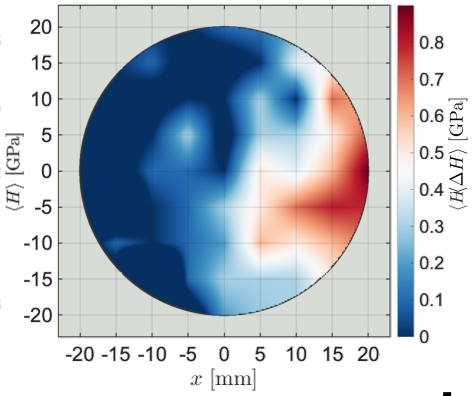

Computational framework

NNIP-based generalized stacking fault energy on HEA system $Co_{0.1}Cr_{0.1}Fe_{0.45}Mn_{0.35}$

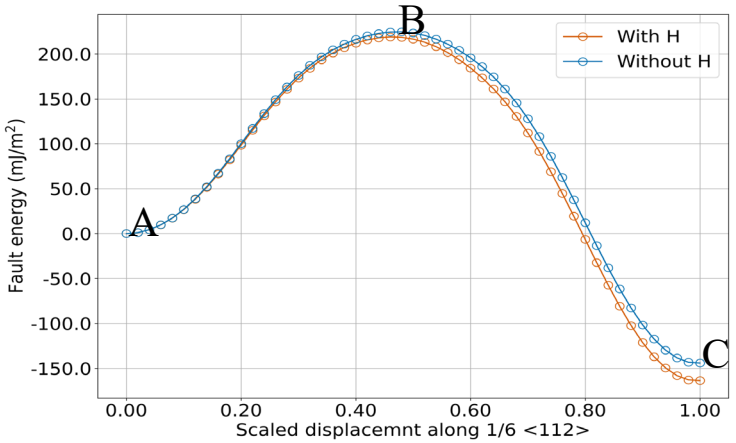

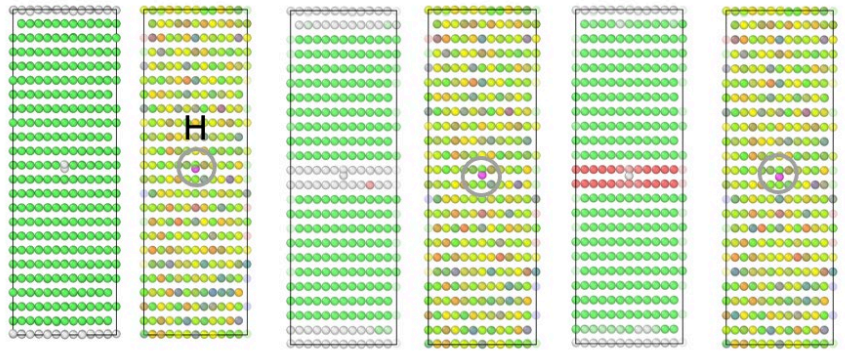

Technical Accomplishments and Progress

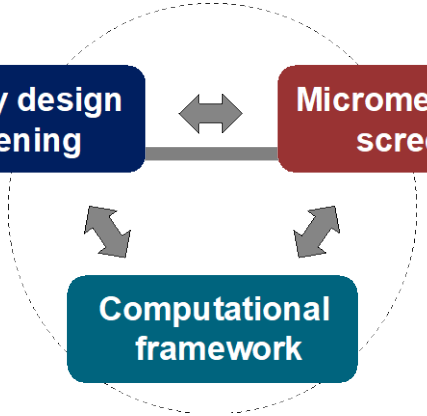

- Our **research progress in the last year of the project** was focused mainly on **identification, production and testing of CCAs** of potential interest and further **computational development**
- Summary of accomplishments (detailed in following slides):
  - ***Methods:***
    1) Fast thermodynamic selection of FeMnCoCr *CCAs based on initial CALPHAD and micromechanics screening
    2) Long-timescale methods for hydrogen diffusion based on off-lattice kinetics MC methods with reinforcement learning
  - ***Materials/Mechanisms:***
    1) Microstructural characterization of selected alloys before deformation
    2) Uniaxial mechanical tests before hydrogen charging of selected alloys
    3) Evolution of phase constitution during deformation via synchrotron X-ray diffraction of selected alloys
    4) Uniaxial mechanical tests after hydrogen charging of selected alloys
    5) Effect of hydrogen on phase transformation kinetics via synchrotron X-ray diffraction of selected alloys
    6) H-charging induced twin-boundary kink migration from hybrid **MD-GCMC using the developed FeMnCoCr-H NNIP
    7) Effects of Full/Partial Slip on Formation Energies of H Interstitials on FeMnCoCr system
    8) Stress Triaxiality Effects on Crack Opening in H-Charged Samples

*CCA: Complex Concentrated Alloy

**MC-GCMC: Molecular Dynamics-Gran Canonical Monte Carlo

Taşan Group

Milestones accomplished

Milestone Schedule							
Milestone #	**Project Milestones**	**Type**	**Task Completion Date (Project Quarter)**				**Progress Notes**
			Original Planned	**Revised Planned**	**Actual**	**Percent Complete**	
4.2	Construct a fracture toughness map in a C-space of metastable CCAs	Milestone	M27			100%	We have identified and studied bulge test and indentation-based methods. However the range of compositions studied never revealed any cracking in the form of thin films, even after hydrogen charging. Hence, we proceeded with additional thermodynamic screening to narrow down interesting compositions and we are proceeding with fracture toughness tests on bulk samples.
6.1	Microstructure characterization of produced alloys	Milestone	M30			100%	We have characterized compositions of interest both via SEM-based and high-energy XRD methods.
7.1	Uniaxial mechanical tests after electrochemical H- precharging	Milestone	M32			100%	We have identified and tested compositions of interest.
End of project goal	I. Use high-throughput strategy to discover at least 3 alloy compositions with potential for superior HE-resistance relative to a low-alloy ferritic steel (X52 steel) and an austenitic stainless steels (Type 316). II. II. Synthesize the discovered alloy compositions in the form of bulk alloys with a dimension ≥ 50 x 50 x 50 mm3. Verify the efficacy of the high-throughput alloy design strategy by demonstrating a bulk metastable CCA with potential for superior HE-resistance at an engineering scale.	End of project goal	M36			100%	I. We have combined high-throughput strategies at the bulk, computational and micromechanics level to identify compositions of interest for complex concentrated alloys. II. We have synthesized the at the bulk scale the discovered compositions and demonstrated the potential for superior HE-resistance in alloys with metastable austenite and HCP martensite, such that martensitic transformation to BCT martensite is delayed to very large plastic deformations.

Technical Accomplishments and Progress:

Thermodynamic screening of FeMnCoCr CCAs

Model prediction of SFE for different compositions of the **FeMnCoCr** system:

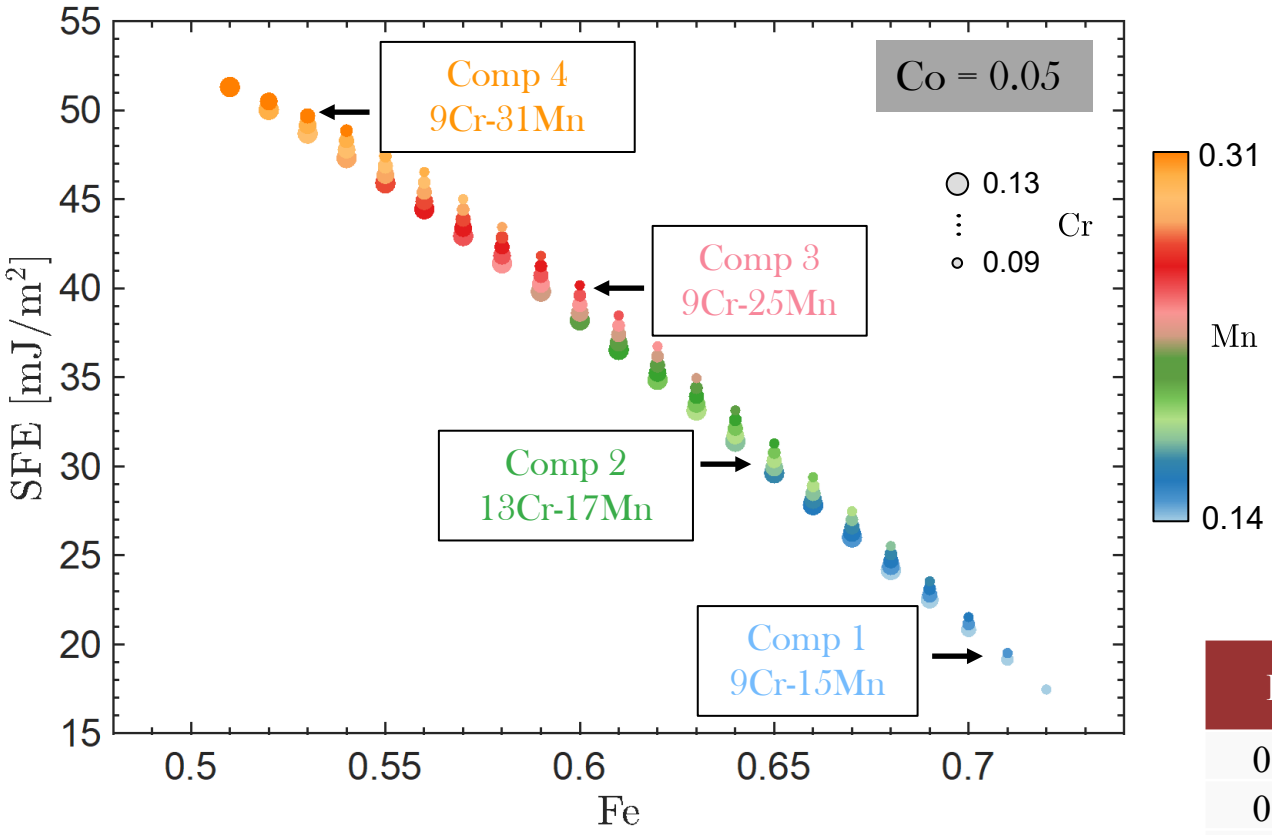

Produced with arc melter + homogenized (1100ºC 3h) + ReX (900ºC 5min)

- Fixed the content of Co to the maximum value of 5 at% (Co tends to increase the SFE).
- Effect of Cr and Mn on SFE is similar.
- All compositions are expected to be single austenitic phase (FCC)
- The austenite is metastable in all cases.

We chose 4 compositions with a range of SFE:

Fe	Cr	Mn	Co	T [K]	SFE [mJ/m²]	M_S [ºC]	Austenite fraction
0.71	0.09	0.15	0.05	300	**19.5**	-30.3	1
0.65	0.13	0.17	0.05	300	**29.6**	-135.9	1
0.61	0.09	0.25	0.05	300	**38.4**	-374.3	1
0.55	0.09	0.31	0.05	300	**48.0**	-580.7	1

Technical Accomplishments and Progress:

Microstructural characterization BEFORE deformation

All samples are predominantly single FCC phase as predicted.

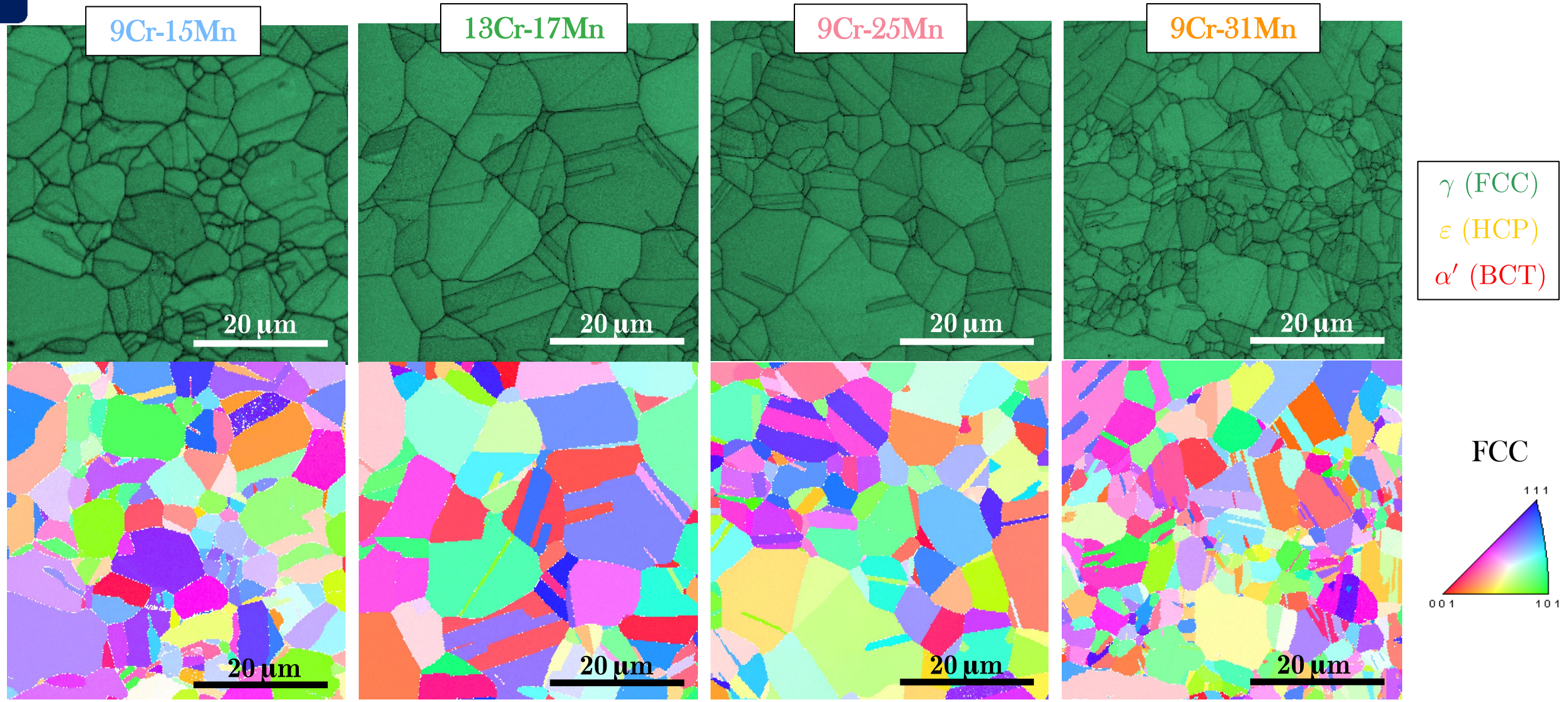

Technical Accomplishments and Progress:

Uniaxial mechanical tests BEFORE hydrogen charging

Engineering stress-strain curves

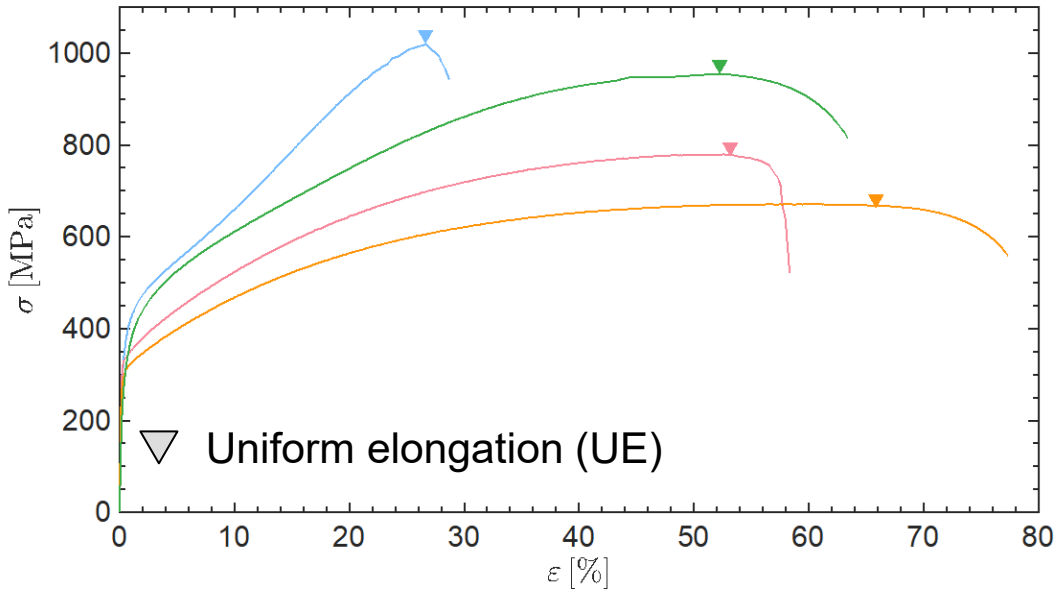

9Cr-15Mn

13Cr-17Mn

9Cr-25Mn

9Cr-31Mn

True stress-strain curves & strain hardening rates

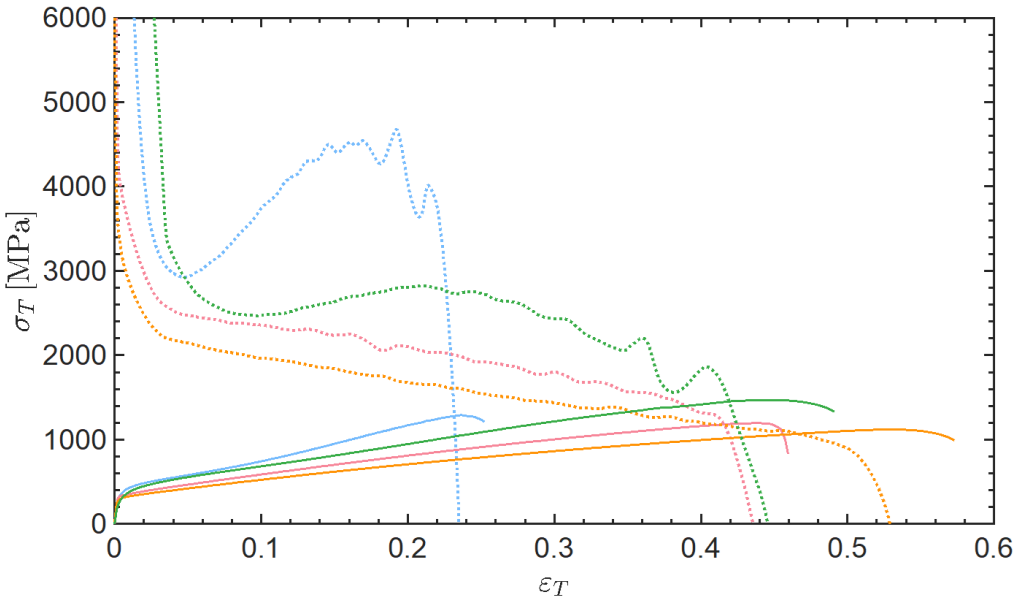

Max UE (%)	UTS [MPa]	0.2% Yield strength [MPa]
27	1015	330
52	954	250
53	778	330
66	667	290

- **Higher Mn** content behaves similarly to other austenitic steels
- **Lower Mn** content shows “second” hardening regime (mechanically induced martensitic transformation) with difference in strain level and magnitude.

→ Kinetics of martensitic transformation?

Technical Accomplishments and Progress:

Evolution of phase constitution with strain: BCT martensite

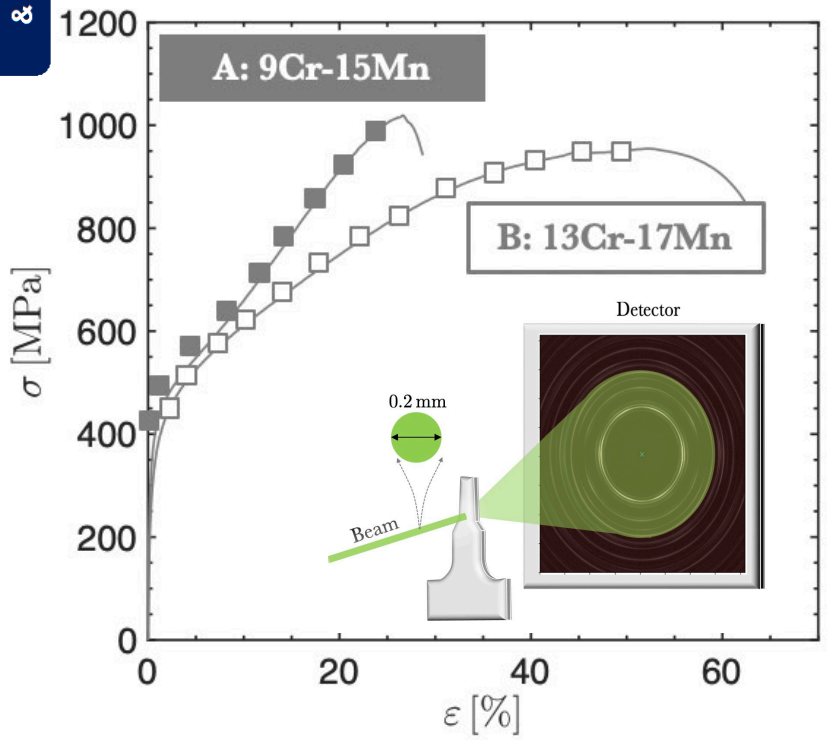

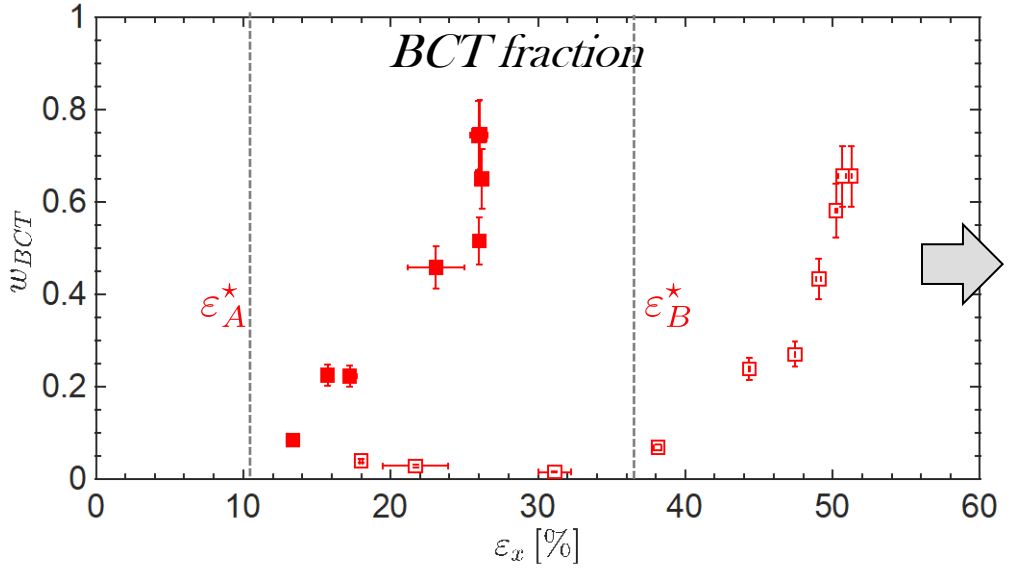

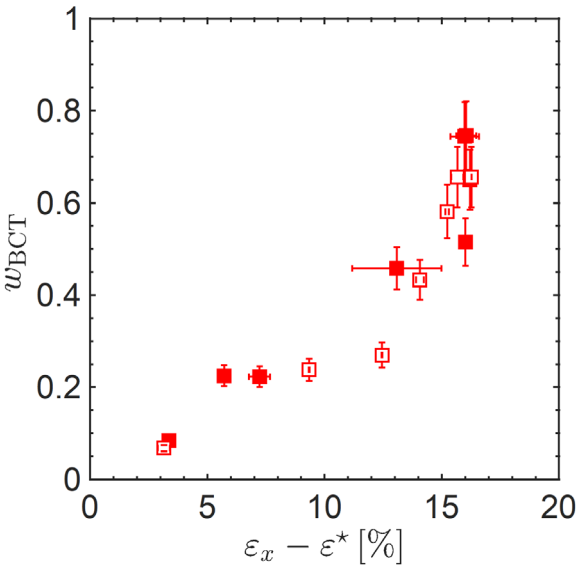

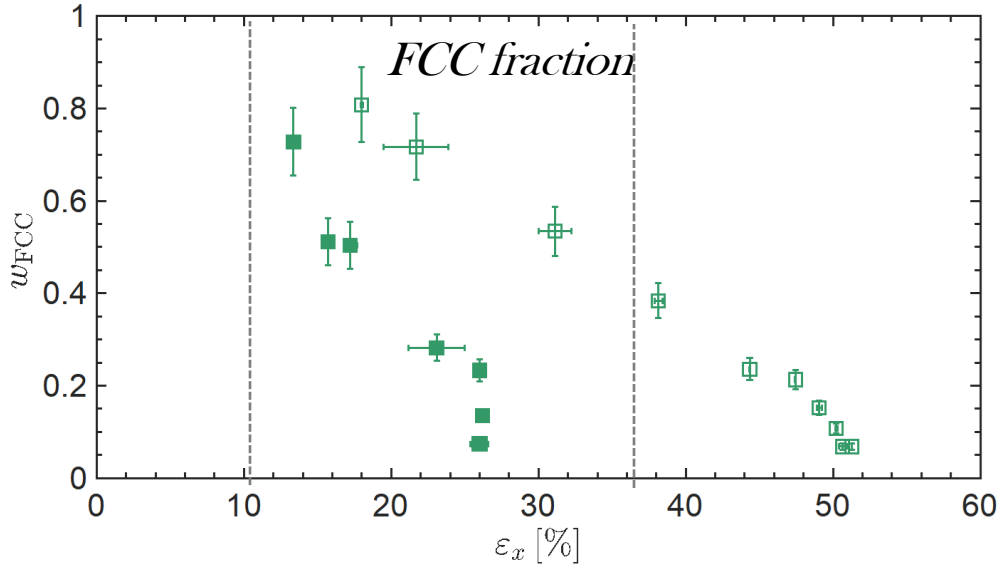

Delayed ε → α' transformation: metastability of ε-martensite
(higher strain energy of activation of phase transformation)

Technical Accomplishments and Progress:

Evolution of phase constitution with strain: role of HCP martensite

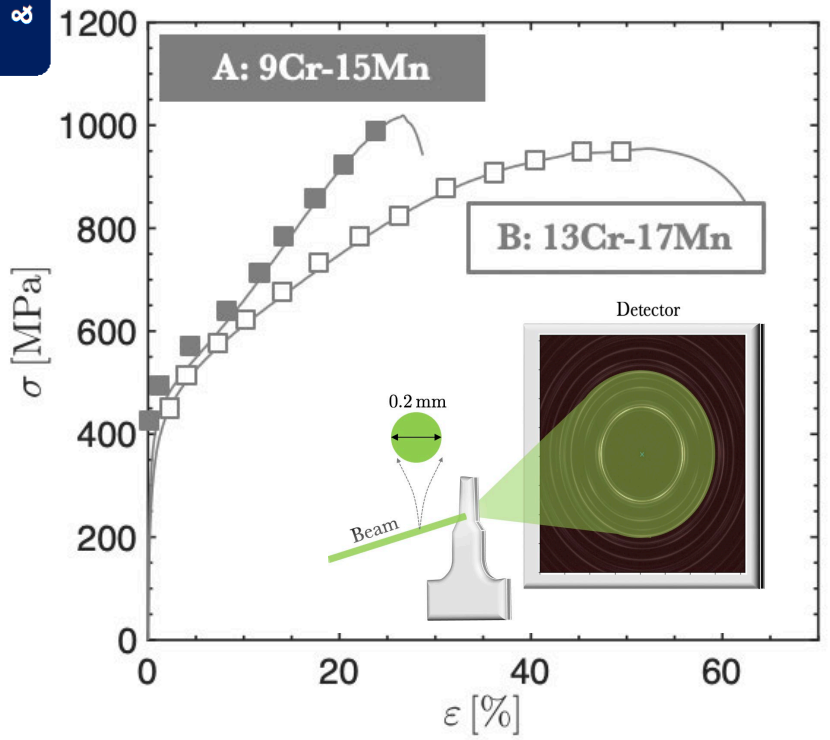

HCP ε-martensite is contributing to strengthening.

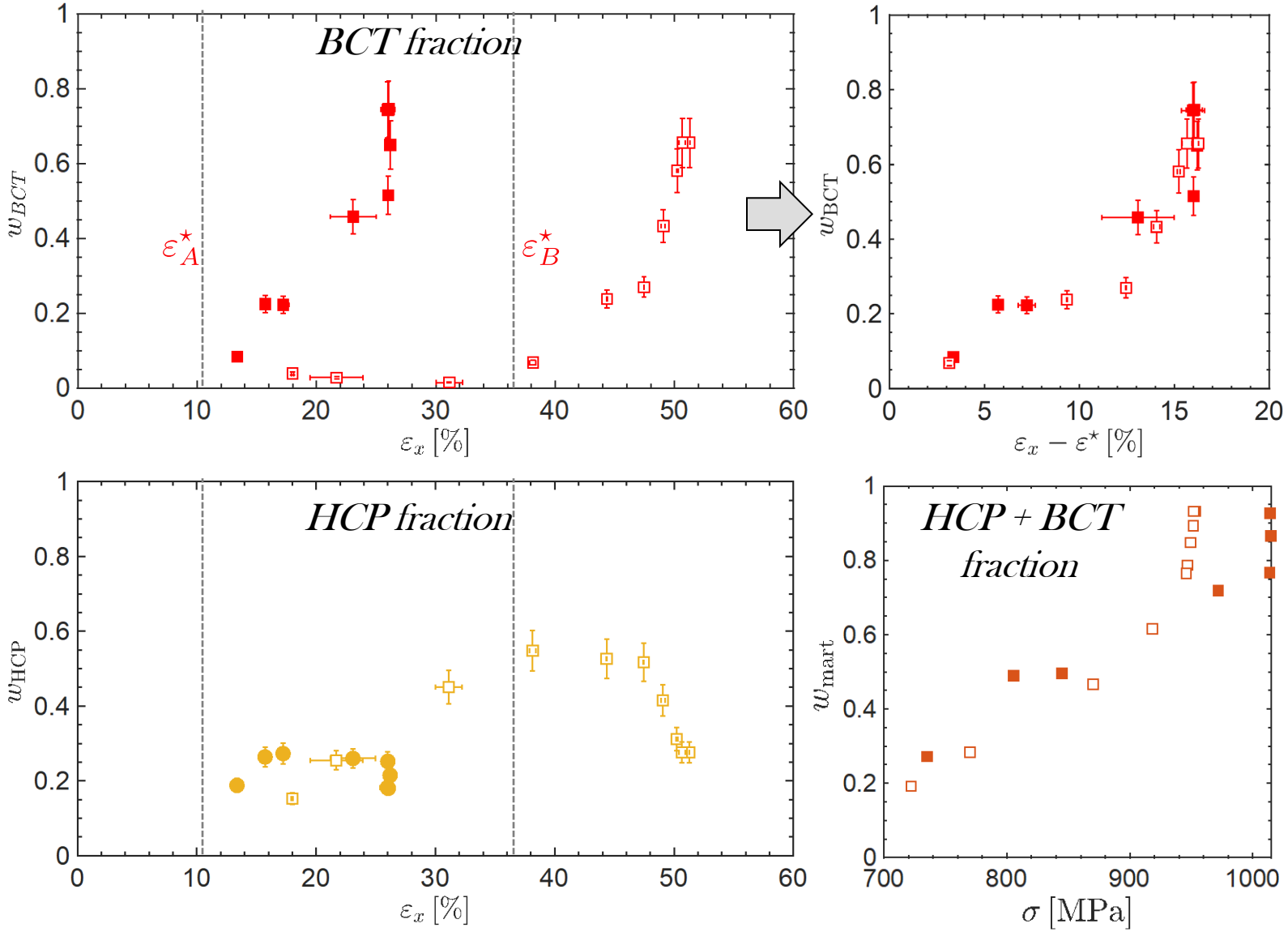

Technical Accomplishments and Progress:

Characterization AFTER hydrogen charging

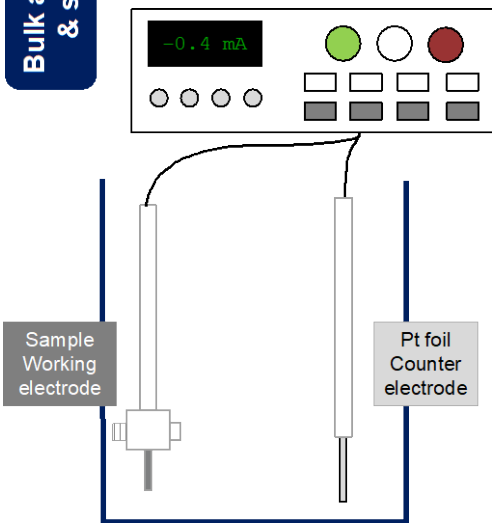

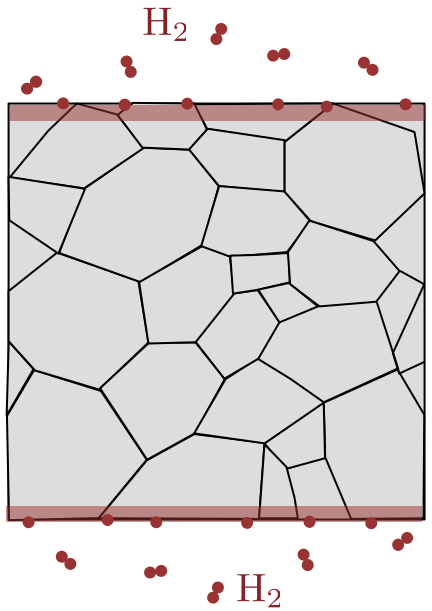

Hydrogen has time to diffuse only in thin layer around sample.

Engineering stress-strain curves

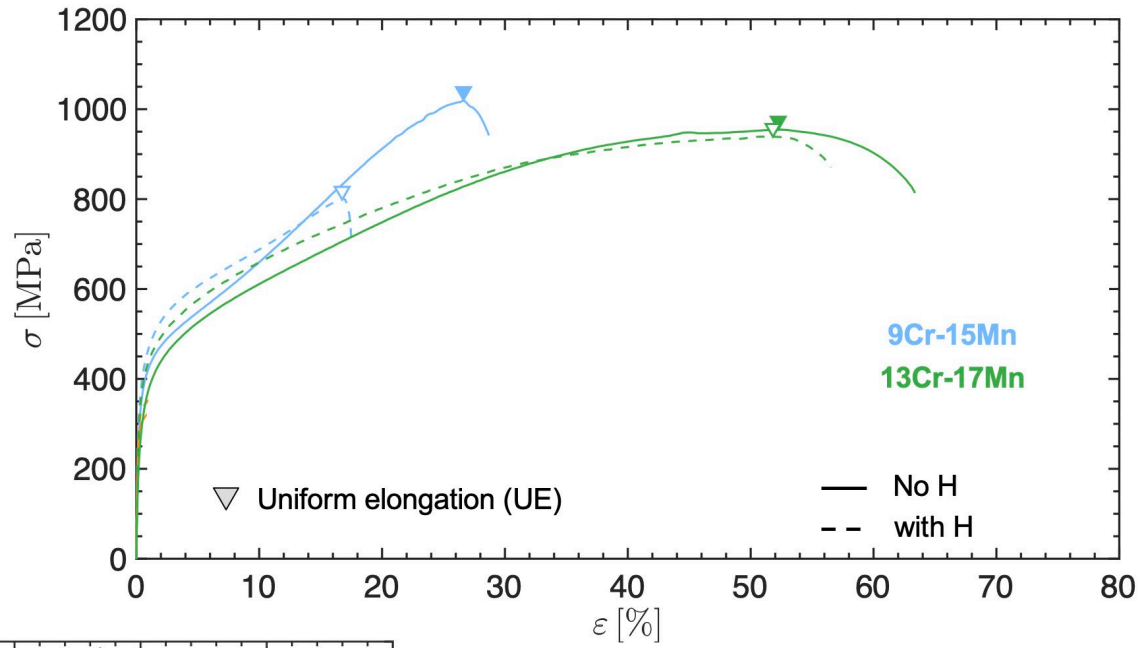

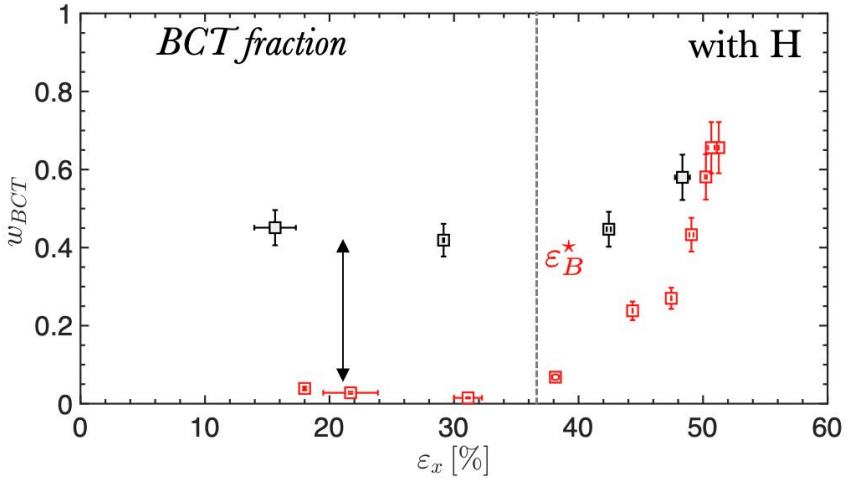

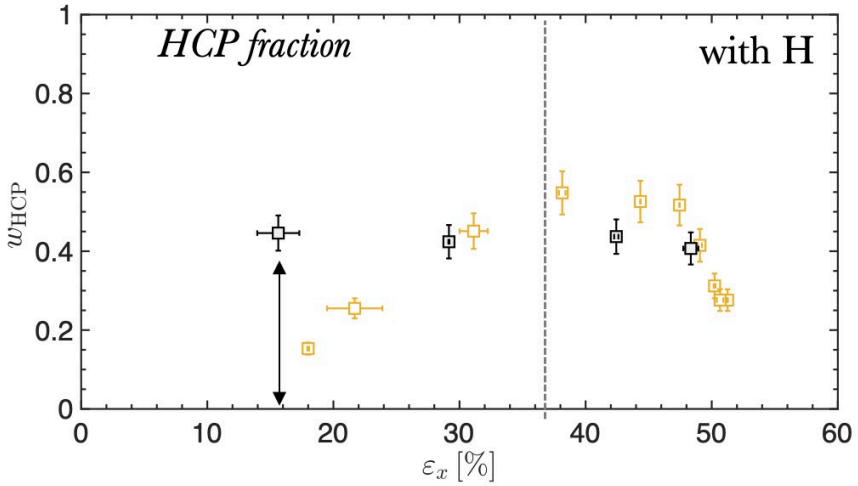

Delayed transformation to α' at larger strains contributes to extended ductility and delayed plastic instabilities.

Technical Accomplishments and Progress:

Hydrogen Charging Induced Twin-Boundary Kink Migration

The following two videos show twin-boundary kink migration under different H chemical potentials, as obtained from hybrid MD-GCMC (Grand Canonical Monte Carlo) Simulations using our CoCrFeMn-H neural network interatomic potential.

H: black atoms
TB: red atoms
FCC: green atoms
TB-kink: grey atoms

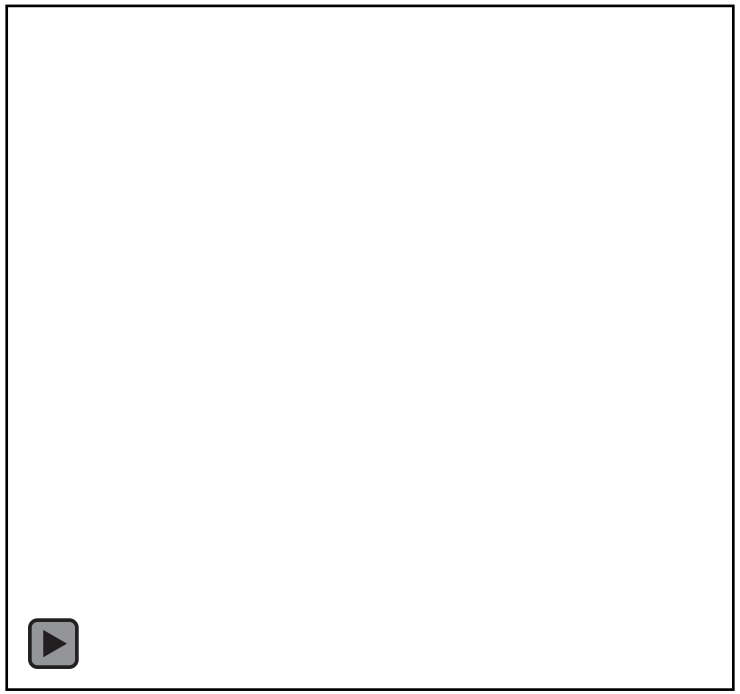

μ_H = -3.0 eV

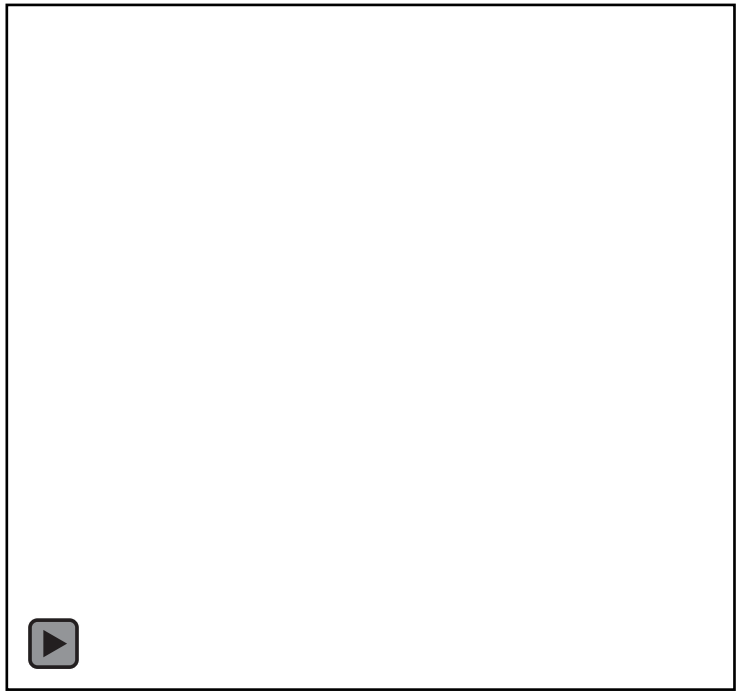

μ_H = -3.5 eV

- A new neural network interatomic potential for the Co-Cr-Fe-Mn-H system was developed
- Hybrid MD-GCMC simulations show that H atoms prefer to stay on the octahedral sites of FCC lattice
- Higher chemical potential leads to higher H atom concentration
- H charging induces twin boundary kink migration

Technical Accomplishments and Progress:

Effects of Full/Partial Slip on Formation Energies of H Interstitials

The H interstitial formation energy distributions in a CoCrFeMn system was investigated using neural network interatomic potential, which is crucial to understanding H effects on microstructure changes.

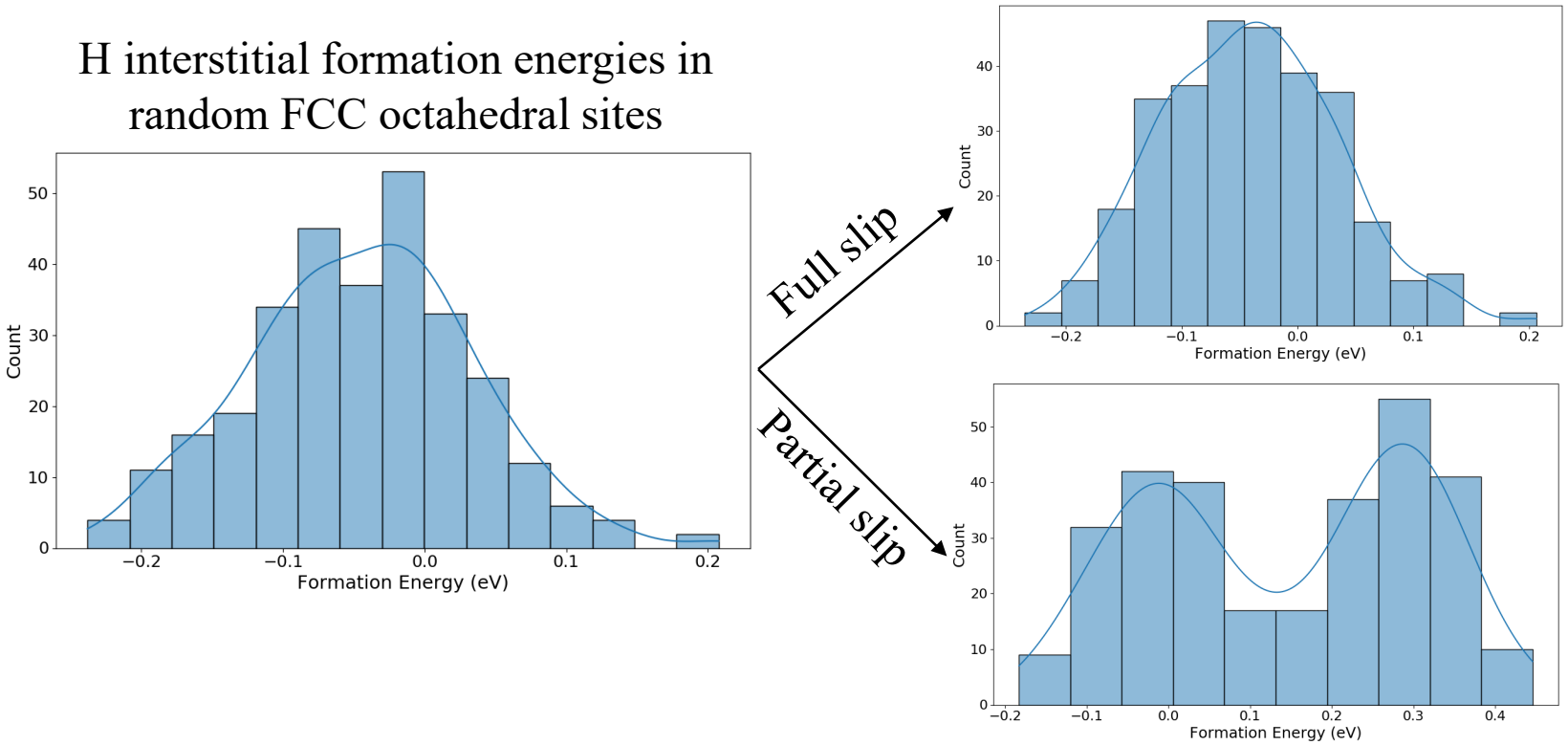

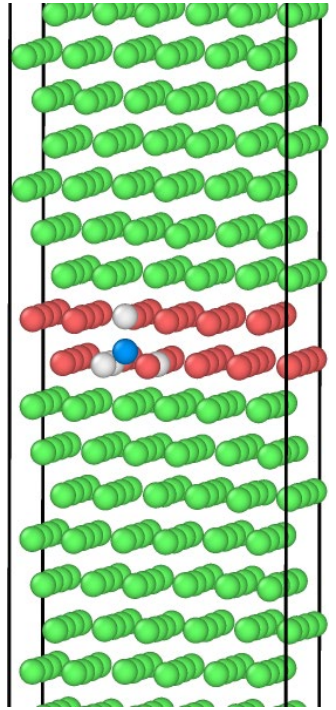

O→T site transformation due to partial slip

- Octahedral H interstitial formation energies form a normal distribution due to random local chemical environments
- Full dislocation slip does not alter the formation energy distribution, but can lead to large formation energy changes
- Partial dislocation slip changes the normal distribution into a bimodal distribution, due to the octahedral to tetrahedral site transformation in the formed stacking fault.

Technical Accomplishments and Progress:

Long-timescale methods for hydrogen diffusion

We developed off-lattice kinetics Monte Carlo methods with reinforcement learning (RL) accelerators that simulates hydrogen diffusion in both single element alloys and multi principal element alloys

1. Begin from s_t
2. Machine learning policy $\pi(a_t|s_t)$ samples a moving direction a_t
3. Guided by a_t, saddle point search algorithm finds adjacent saddle point s_t^*
4. Relax the system from s_t^*, obtaining the next step s_{t+1}
5. Obtaining reward $r_t = \alpha(E_t - E_t^*) + \beta(E_t - E_{t+1})$
6. Train the policy $\pi(a_t|s_t)$ to maximize reward

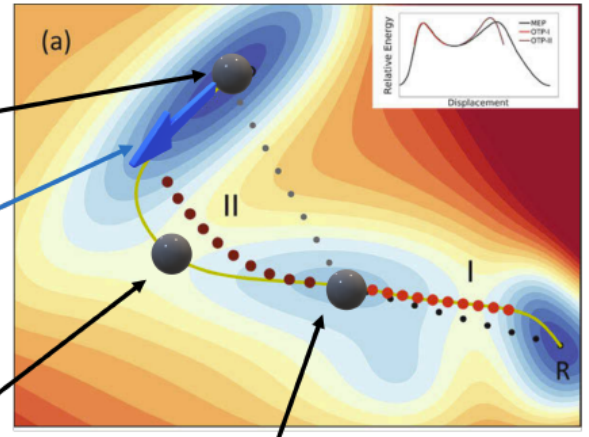

1. Equivariance graph neural network empirical potential
2. Minimum mode follow method for transition

$$F_{\text{eff}} = -\nabla U + 2(\vec{e}_{\min} \cdot \nabla U)\vec{e}_{\min}$$

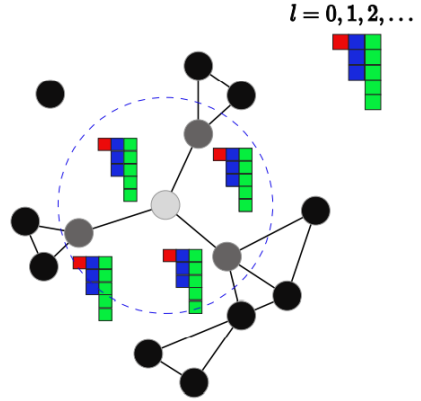

3. Action space: convex hull algorithm to identify polyhedral face center
4. RL: DeepPot descriptor and deep Q network algorithm

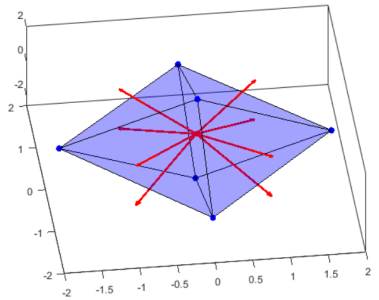

- We develop a simulation package for long timescale H diffusion that can extend the simulation to ms scale
- Reinforcement learning method is used to accelerate calculations
- We studied H diffusion in Cu, Al, and NiCrCo alloy.

Technical Accomplishments and Progress:

Numerical performance of the long-timescale method

structures

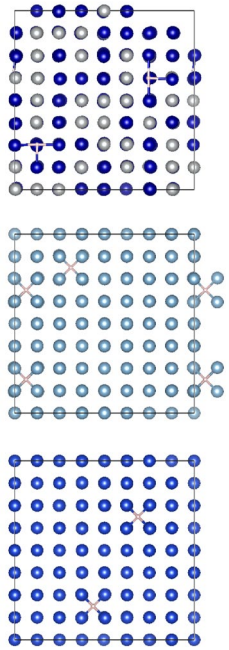

Training: using neural network to predict transition energy barriers

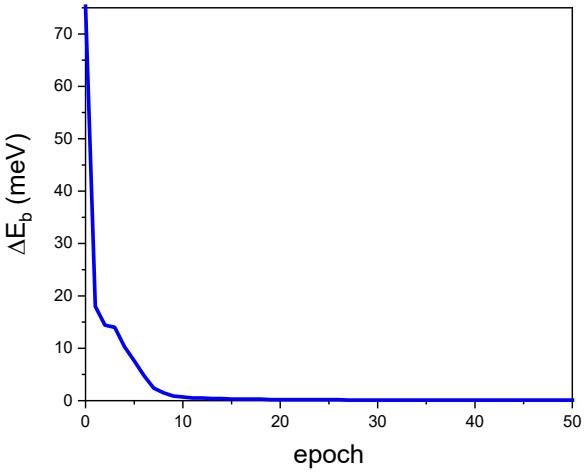

Results: finding minimal barrier transition pathways (MTP)

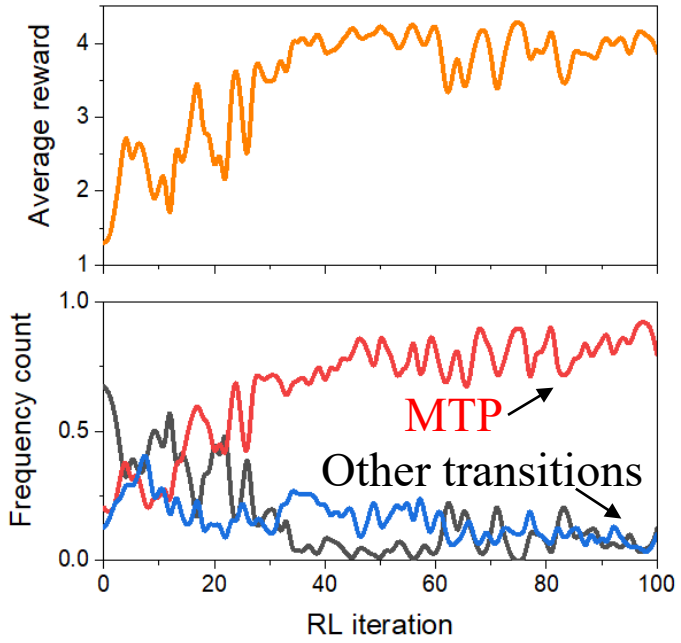

Performance: better efficiency in energy relaxations

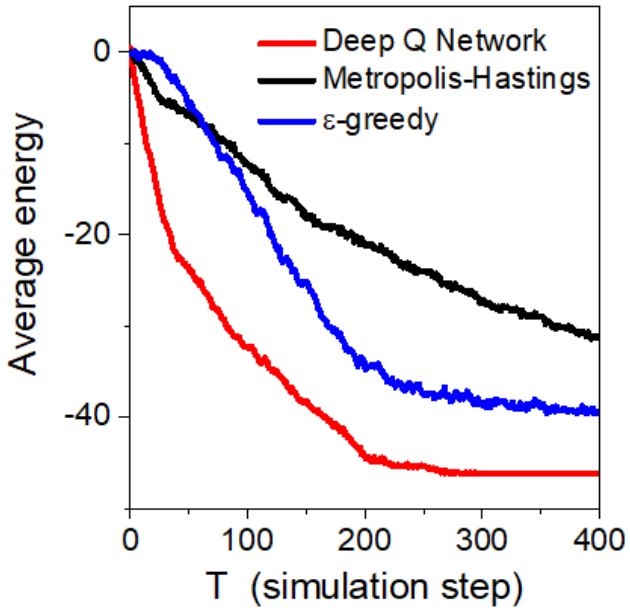

- The models accurately predicts transition energy barriers
- Transition pathways with minimal energy barriers are correctly identified
- Our method is more efficient in simulating long timescale annealing process than traditional Monte Carlo methods.

Responses to 2021 Reviewers' Comments

- Our project was not reviewed during the last AMR, but was reviewed in 2021.

- *Comment 1* - The project should include details of the next-level characterization of HE behavior and considerations of multi-properties.

Since the last review we have moved from thin film to bulk scale production and characterization of the alloys of interest, which we selected with a combination micromechanical and thermodynamic approaches. We have proceeded with a complete characterization of the alloys both in the absence and in the presence of hydrogen (see slides 10-15). Our selected alloys can be easily bulk produced and thermo-mechanically processed (very good ductility and formability, short heat treatments). Also, given the lower Mn content compared to other alloys that show good HE resistance, they have the potential to become competitive in terms of cost.

- *Comment 2* - It is recommended that the project include industry stakeholders in hydrogen technology as project partners.

ATI has been a partner of the project, participating in the first 1.5 years of update meetings and discussions.

Collaboration and coordination

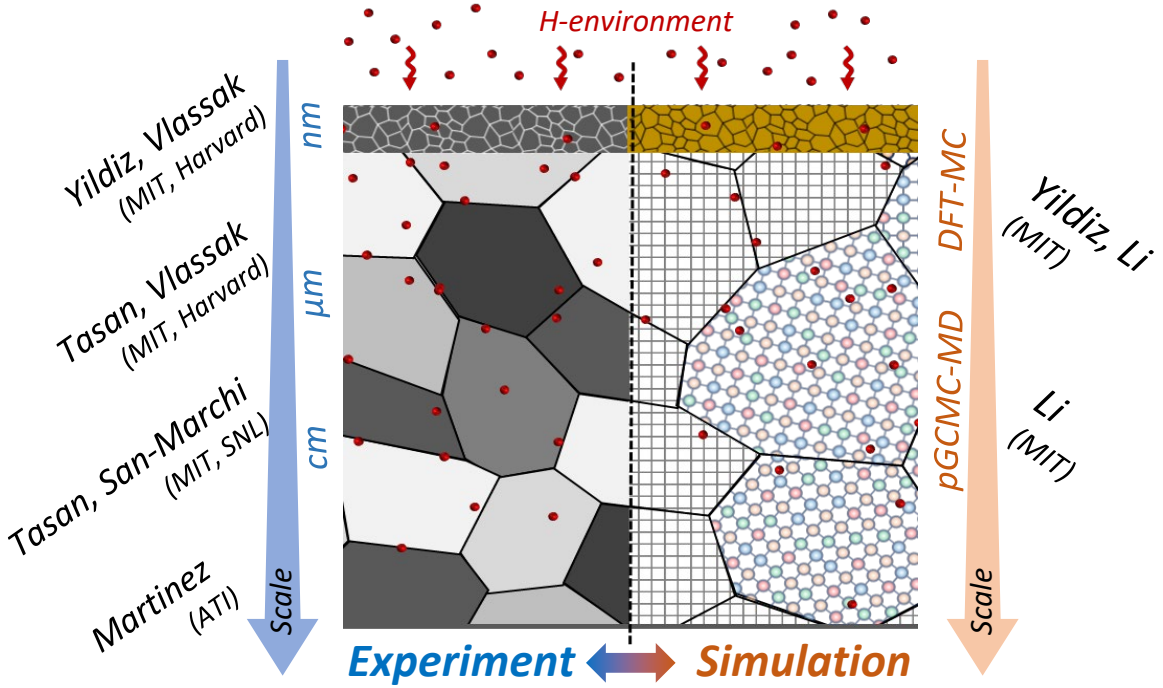

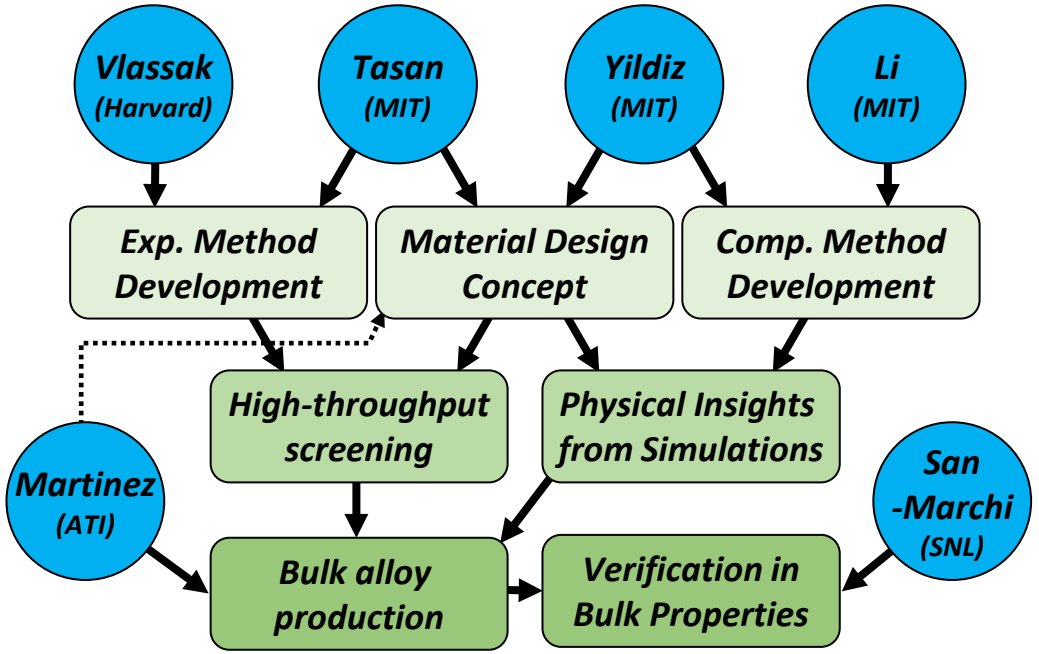

Team members and partners	Project roles
Tasan Group, MIT	Project lead, Management/coordination, Setup design, Alloy design, Experimental methodology development, Bulk alloy production
Li Group, MIT	Computational technique development, Interatomic potentials development
Yildiz Group, MIT	Surface structure and property characterization, Computational technique development,
Vlassak Group, Harvard University	Composition spread film fabrication, Heat treatment, Micromechanical testing, Experimental methodology development
ATI (Unfunded industrial partner)	Bulk alloy production, Consultant on alloy system selection, production and industrial requirements
Sandia National Lab. (H-Mat partner)	Bulk alloy testing in high-pressure hydrogen environment (planned for Year 3)

Possible Future work

- **Materials:**
  - Investigate alloys with similar stacking fault energy to those of interest (around 30 mJ/m^2) but different compositions to study more in depth the role of metastable ε-martensite.
  - Develop predictive capabilities for transformation kinetics from ε- to α´-martensite with appropriate thermodynamic theory to aid future alloy design.
- **Methods:**
  - Extend the NNIP trained by DFT calculation to all magnetizations; Apply the potential to study magnetic properties of multi-element alloy controlled by compositions, temperature, and pressure through MD simulations.
  - Combine active learning, hybrid MD-GCMC (Grand Canonical Monte Carlo) simulations, and first-principles calculations to systematically generate a large data set that can be used to address defects-H interactions with and without chemical short-range ordering.

Any proposed future work is subject to change based on funding levels.

Summary

- ***Methods:***

  – By combining high-throughput screening of large compositional spaces of CCA via thermodynamic simulations and micromechanical testing we have been able to identify interesting alloy compositions with potential for metastability-induced HE-resistance.

  – We established a spin-aware neural-network-based interatomic potentials for complex concentrated alloys and used to understand the role of hydrogen at grain boundaries as well as the role of hydrogen on stacking fault energy. A magnetic interatomic potential for multi-element alloys has also been developed and tested.

  – A simulation framework to study native oxides has also been established and tested with respect to the Al2O3/Al interface as a base for future studies on an Fe-Cr like the HEA used in this study.

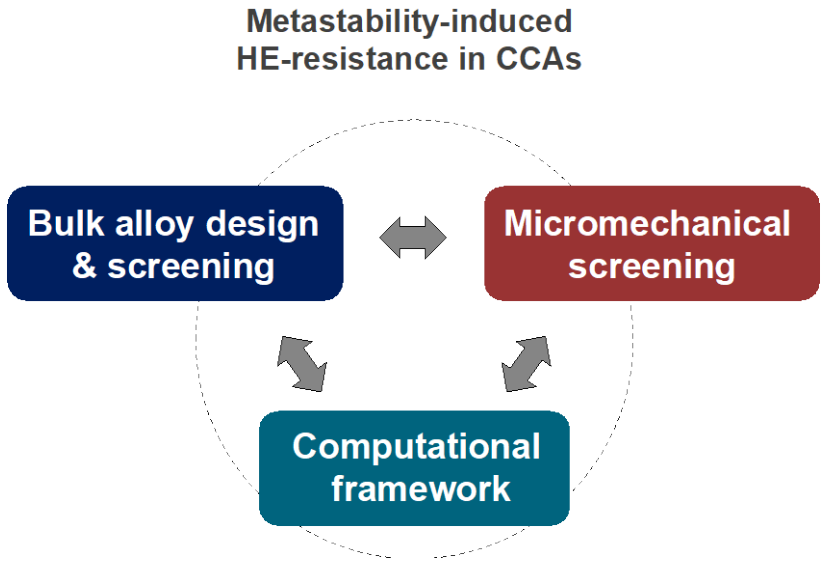

- ***Materials/Mechanisms:***

  – Bulk-production and testing of the compositions of interest revealed the important role of metastable ε-martensite, especially when its transformation to α´ is delayed to very large plastic strains. This allows to combine the benefits of hardening via deformation induced martensitic transformation and good hydrogen resistance.

  – The effects of H on microstructural changes are supported by the spin-aware neural-network-based interatomic potentials for CCAs. H charging leads to stacking fault and HCP phase formation. Our calculations suggest a reduction of intrinsic SFE with addition of H. Decreased SFE due to H can be a driving force for experimentally observed phase transformation.

Technical Backup and Additional Information

Technology Transfer Activities

- We explored a wide range of compositions during the alloy design process, considering the scalability of the processing, and the resulting property benefits.

- The project team also interacted with the unfunded industrial partner, ATI. Alloy manufacturing and application experts from ATI has joined the progress update meetings and sharing opinions on alloy system selection and industrial requirements.

- Next step is exploring alloy design possibilities to transfer the observed mechanisms to commercial systems.

Presentation and Publications

- ***Presentations:***

  i. M. Geri, M. Jiang, C.C. Taşan, Materials Science and Engineering (MSE) Congress 2022, Darmstadt and Online, September 2022 “In-situ SEM micro-mechanical testing to unravel hydrogen embrittlement mechanisms in high strength alloys”

  ii. M. Geri, C.C. Taşan, Alloy Design Workshop, MIT (& streamed online), December 2nd 2022 “Exploring the Benefits of Metastability Against Hydrogen Embrittlement”

  iii. M. Geri, M. Jiang, C.C. Taşan, TMS 2023, March 2023 “Unraveling hydrogen embrittlement of model high entropy alloys”

  iv. C.C. Taşan, H.S. Oh, M. Geri, M. Jiang, (invited) TMS 2023, March 2023 “Hydrogen embrittlement in alloys with metastable phases”

- ***Publications:***

  i. Ronchi, M. R., H. Yan, and C. C. Tasan. "Hydrogen-Induced Martensitic Transformation and Twinning in Fe 45 Mn 35 Cr 10 Co 10." Metallurgical and Materials Transactions A (2021): 1-17.

  ii. Somjit, Vrindaa, and Bilge Yildiz. "Atomic and Electronic Structure of the Al2O3/Al Interface during Oxide Propagation Probed by Ab Initio Grand Canonical Monte Carlo." ACS Applied Materials & Interfaces 14, no. 37 (2022): 42613-42627.

  iii. Tang, Hao, Yin Zhang, Qing-Jie Li, Haowei Xu, Yuchi Wang, Yunzhi Wang, and Ju Li. "High accuracy neural network interatomic potential for NiTi shape memory alloy." Acta Materialia 238 (2022): 118217.

  iv. M. Geri, M. Jiang, C.C. Taşan, “Role of metastability in the design of hydrogen embrittlement resistant alloys”, in preparation, 2023

Approach: *CALPHAD-based bulk alloy high-throughput screening*

CALPHAD-informed composition selection → **Alloy production, Thermomechanical processing** → **"Binary" testing: Go/no-Go decision** → **Evaluate results, Identify trends**

- Key focus: maximizing range of microstructures
  - Cast a small number of compositions, post-process to vary microstructures
- Adapted from other alloy design routes:
  - Rapid alloy prototyping
  - Iterative approaches based on machine learning
- Goal: explore HE dependence on phase constitution & transformations in CCAs
  & provide composition ranges to be explored by micromechanical approach in detail

Approach: *Micromechanics-based high-throughput screening*

Bulk alloy testing -informed composition range selection → **Fabrication of composition spreads (Composition library)** → **Rapid property screening with *in situ* H-charging** → **Identify trends from property maps, Verify in bulk scale**

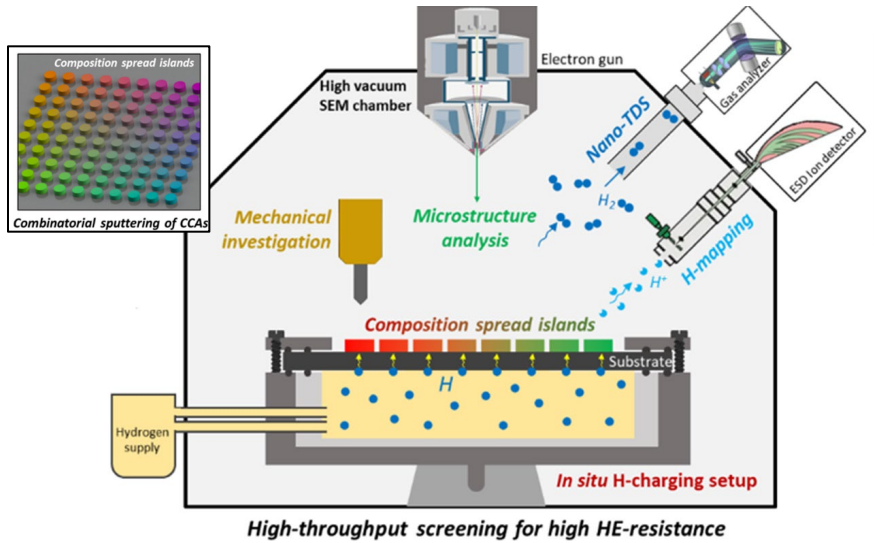

High-throughput screening for high HE-resistance

- Key focus: Rapid property screening on composition spreads
- Property mapping using micromechanical tests
  - *In situ* H-charging indentation-based approach
  - Metastability mapping by H & stress-induced change
- Goal: explore H & deformation-induced microstructural change depending on alloy compositions and phase metastability

Approach: *Computational framework for complex alloys*

Workflow of multicomponent interatomic potential development

Deep-potential generator (DP-Gen): concurrent learning scheme

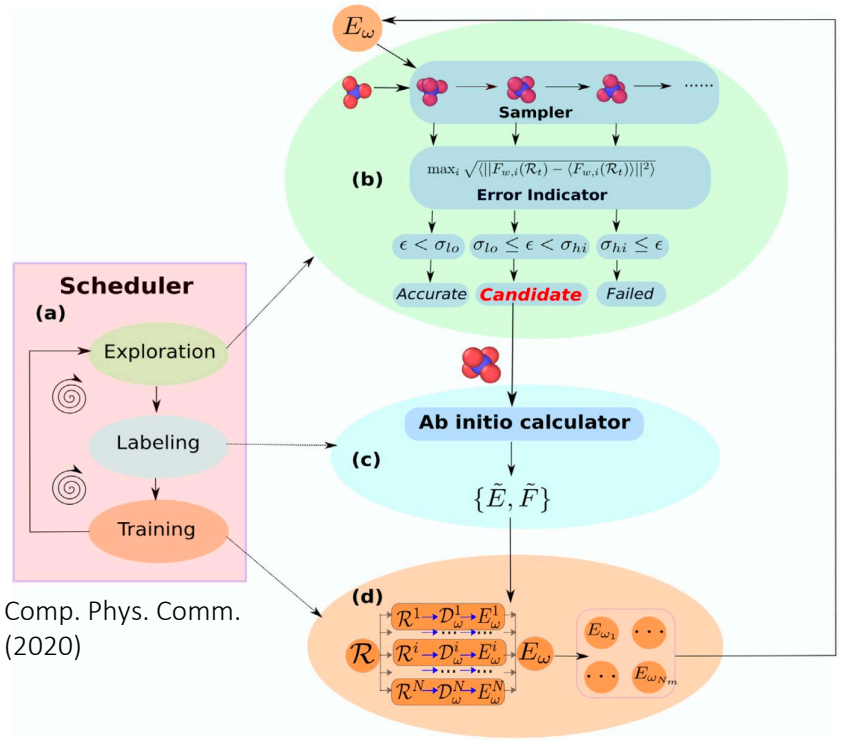

Comp. Phys. Comm. (2020)

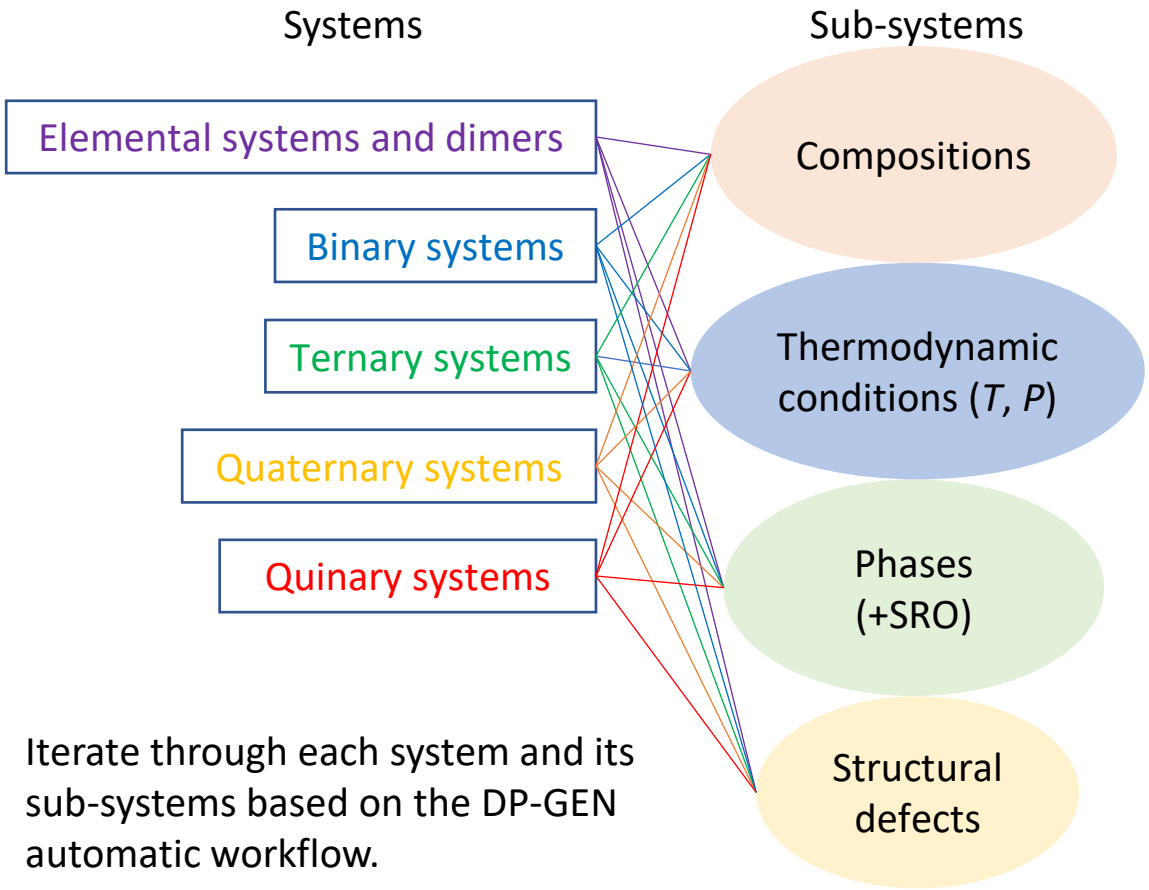

Iterate through each system and its sub-systems based on the DP-GEN automatic workflow.

- Key focus: Establish computational framework for exploring complex multicomponent alloys
- Goal: Bridging the gap between bulk and microscale studies, mainly induced by defect structures

Synchrotron XRD for phase constitution

Data collection

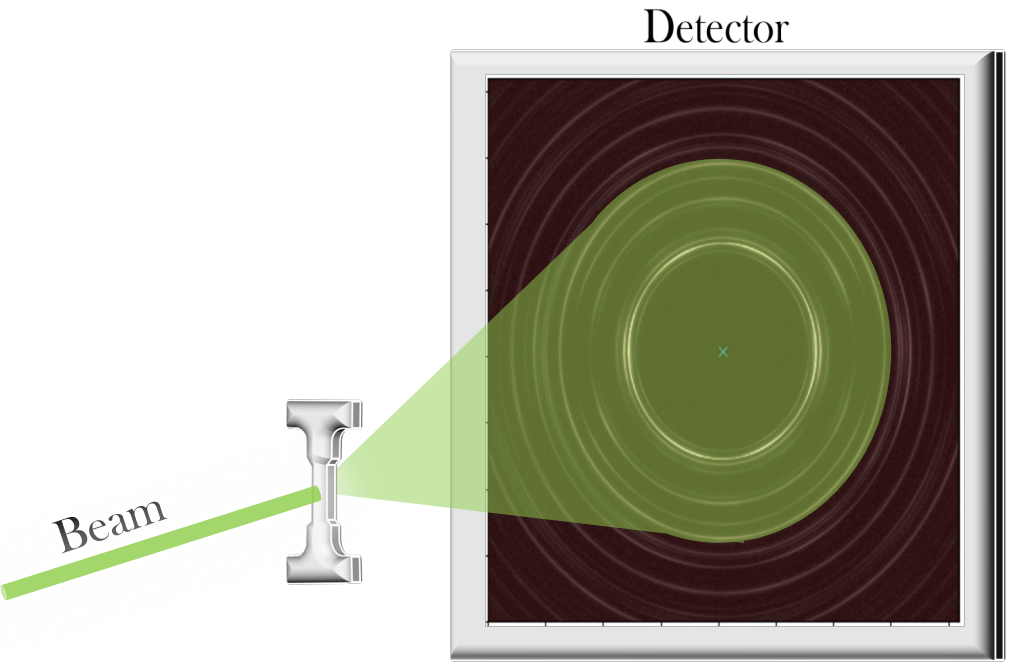

APS Synchrotron (Chicago) beam 11-ID-C

Integration and analysis

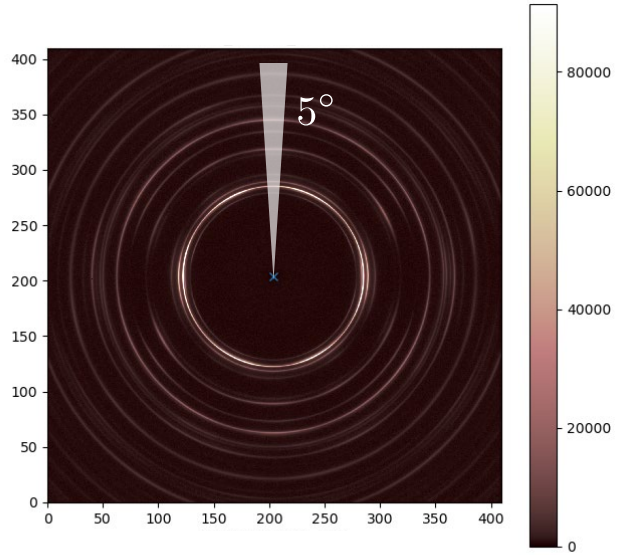

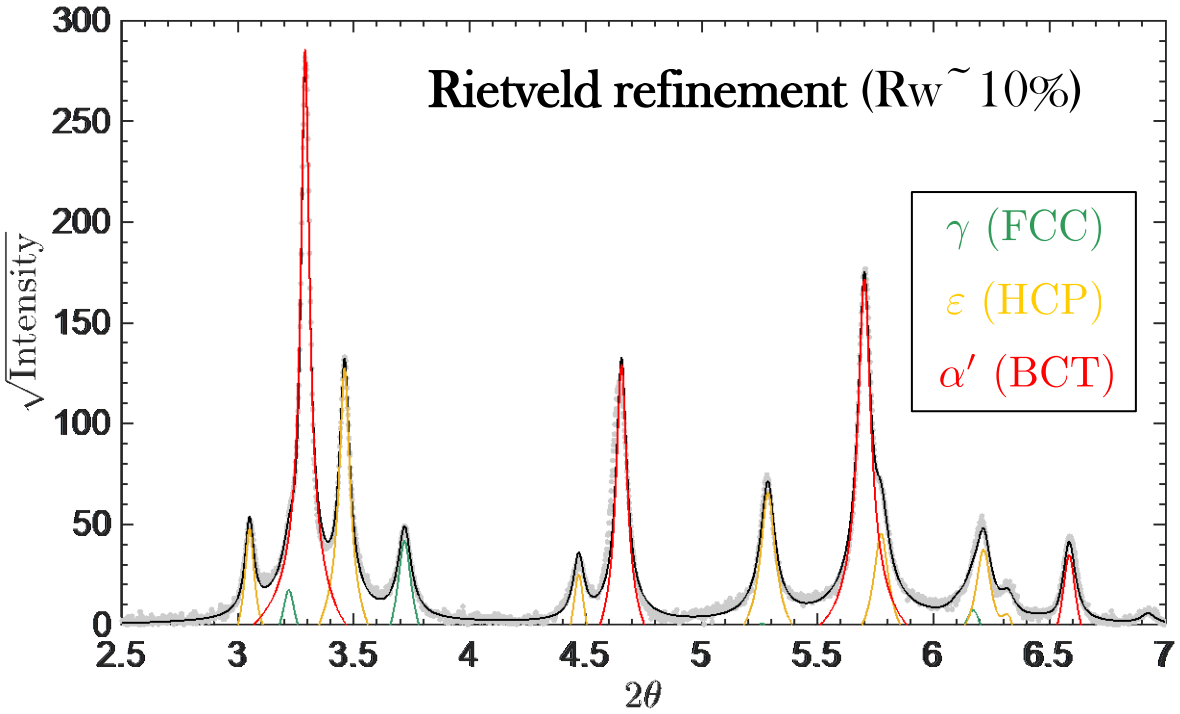

Extracting phase constitution with strain

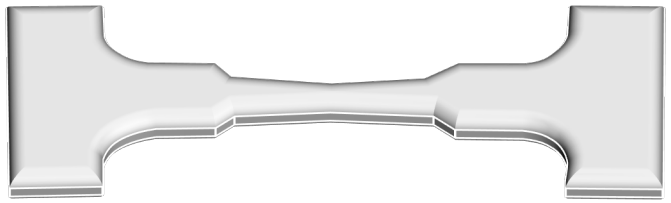

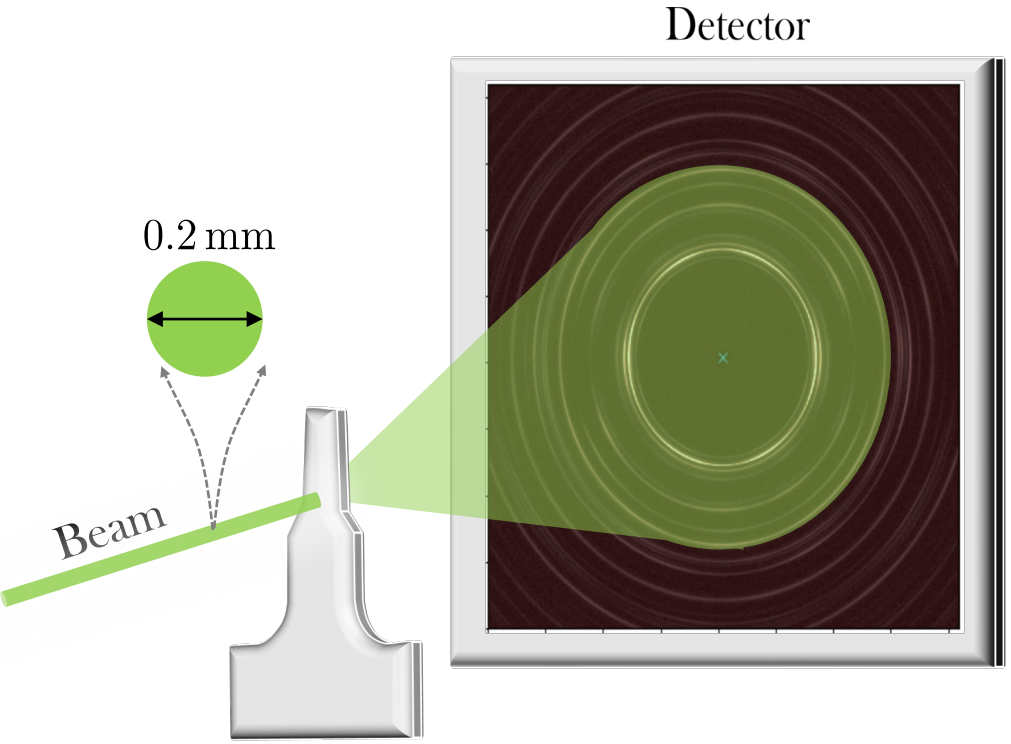

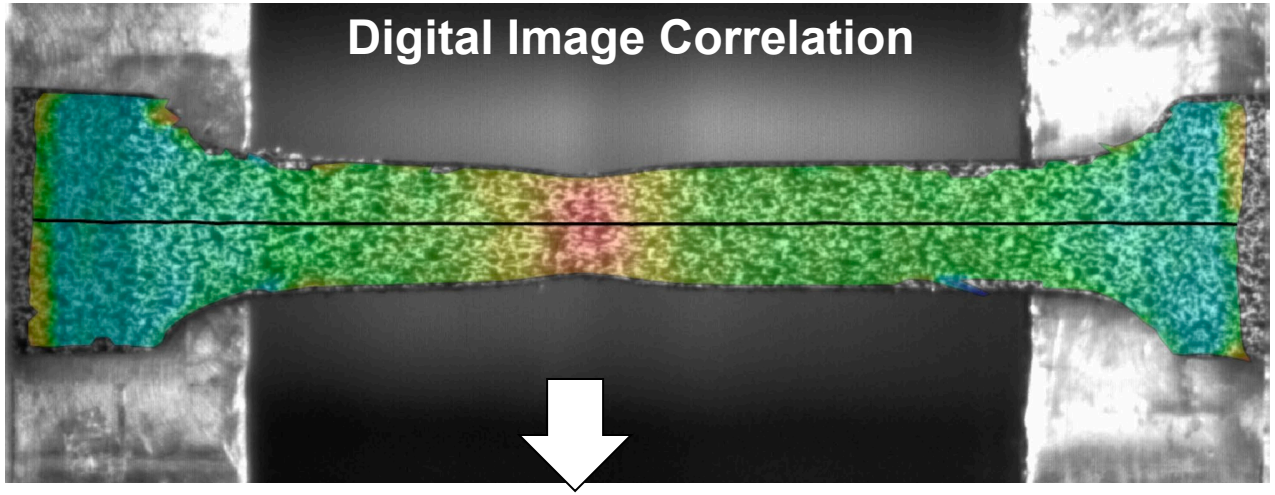

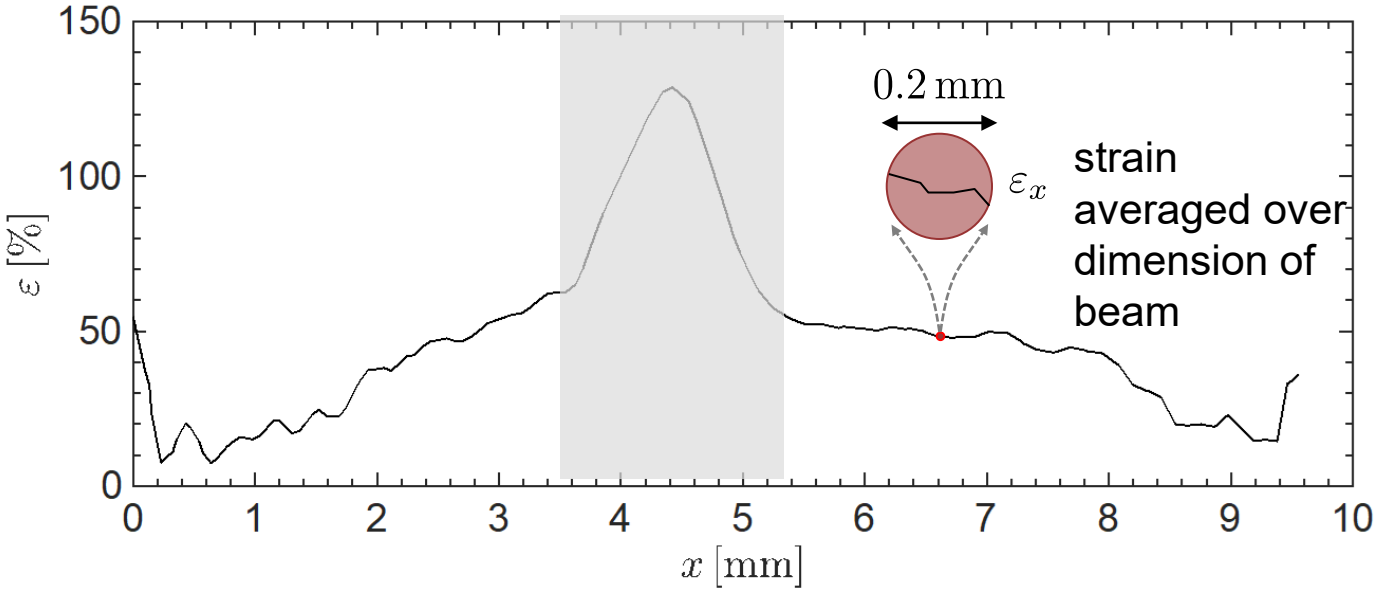

Cathodic hydrogen charging

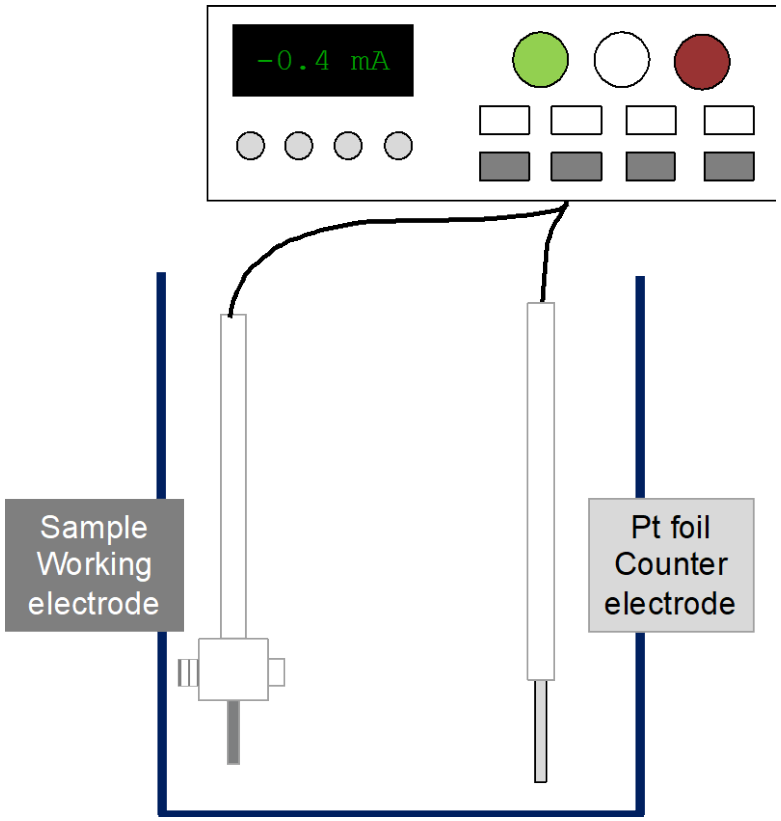

Cathodic H charging:

- **3% NaCl + 3g/L NH_4SCN**
- **24h** charging at **5 A/m²**
- Area to be charged measured optically
- Expected thickness of penetration: ~30-50 μm into external surface

Cross sectional view

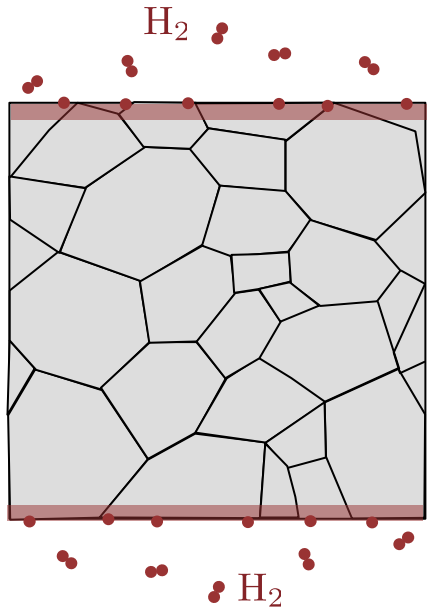

Hydrogen has time to diffuse only in thin layer around sample.

In-situ synchrotron charging

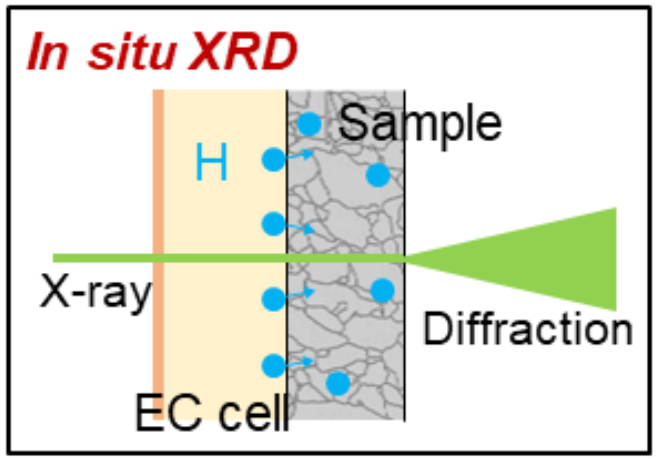

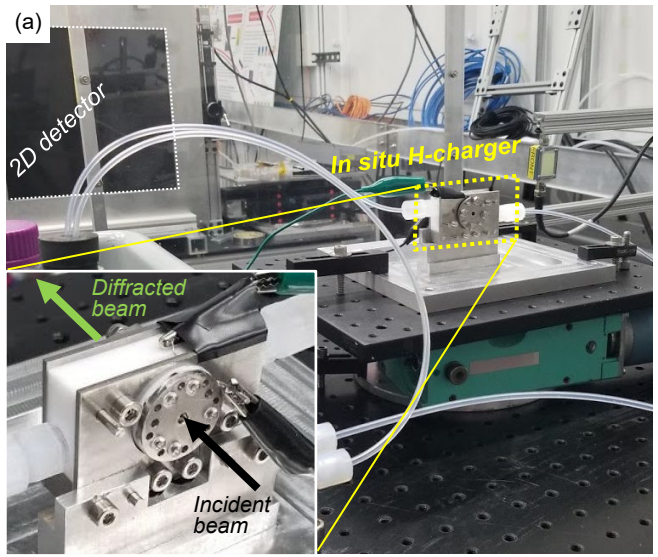

APS Synchrotron (Chicago) beam 11-ID-C

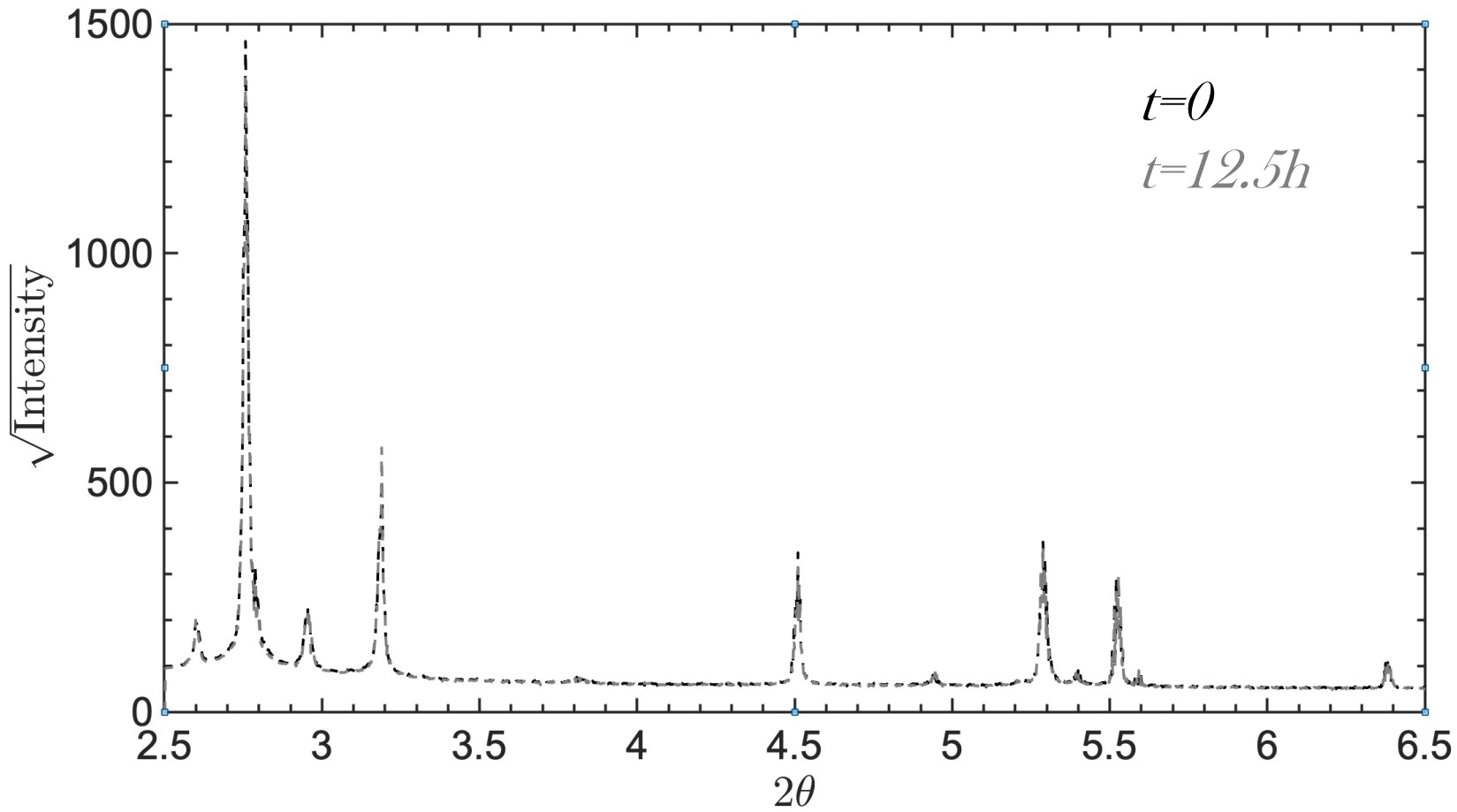

No evident H-induced martensitic transformation over 12.5h

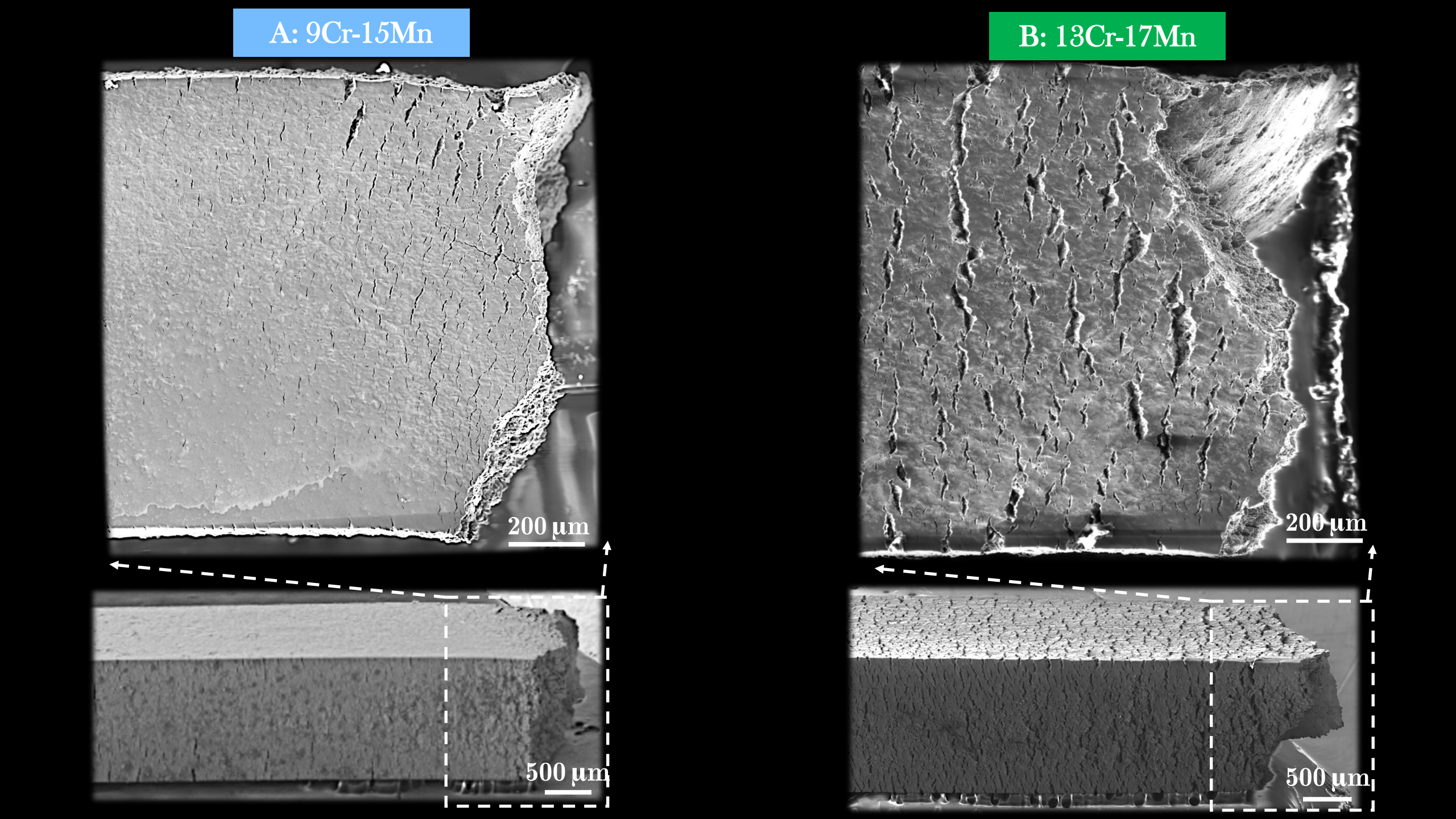
A: 9Cr-15Mn
B: 13Cr-17Mn
200 μm
200 μm
500 μm
500 μm

Effect of hydrogen on phase transformation in 13Cr-17Mn

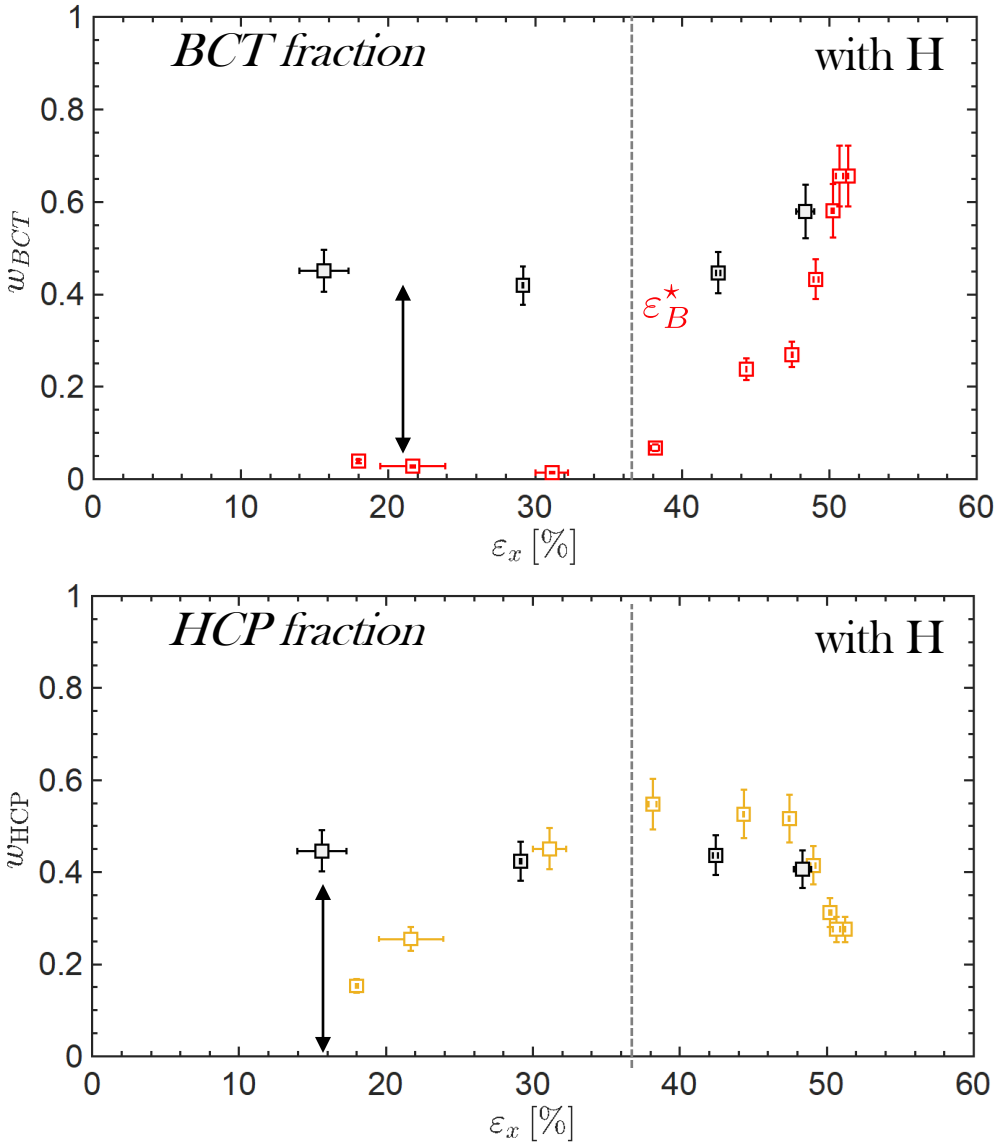

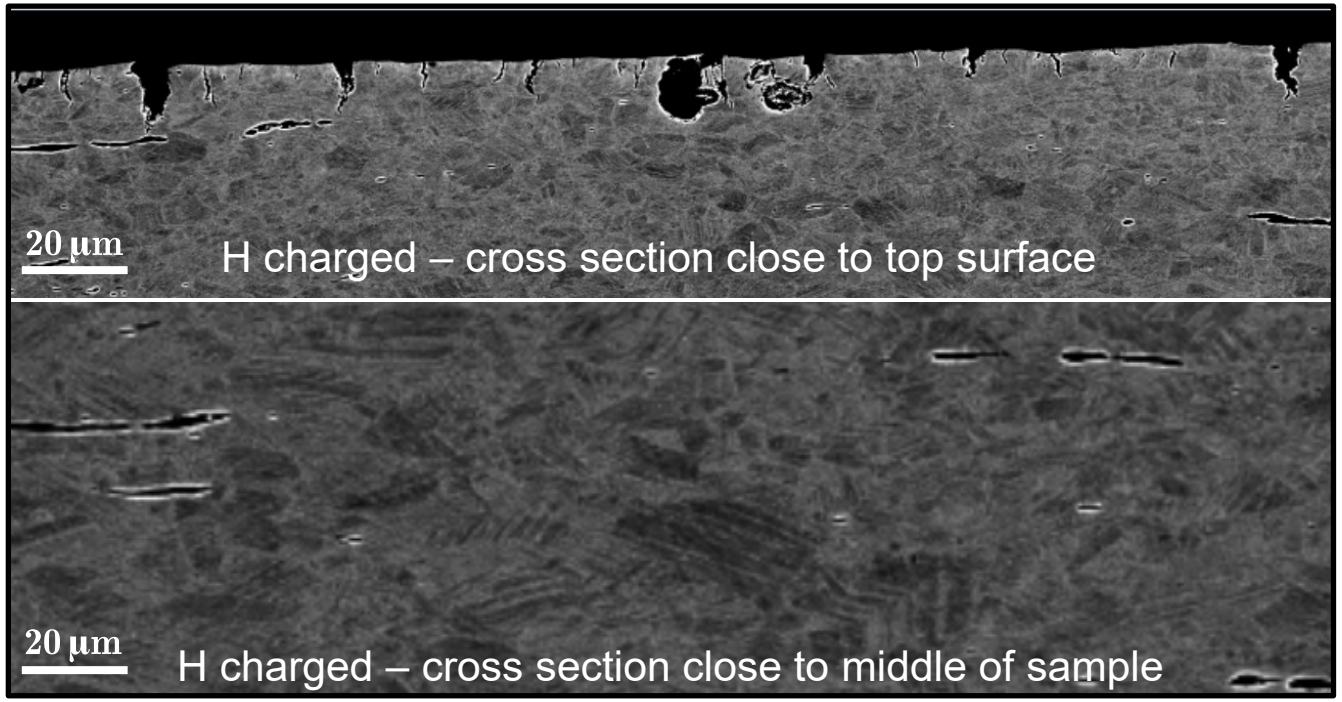

Delayed transformation to α' at larger strains contributes to extended ductility and delayed plastic instabilities.

Metastability of ε HCP: “new” promising tuning parameter

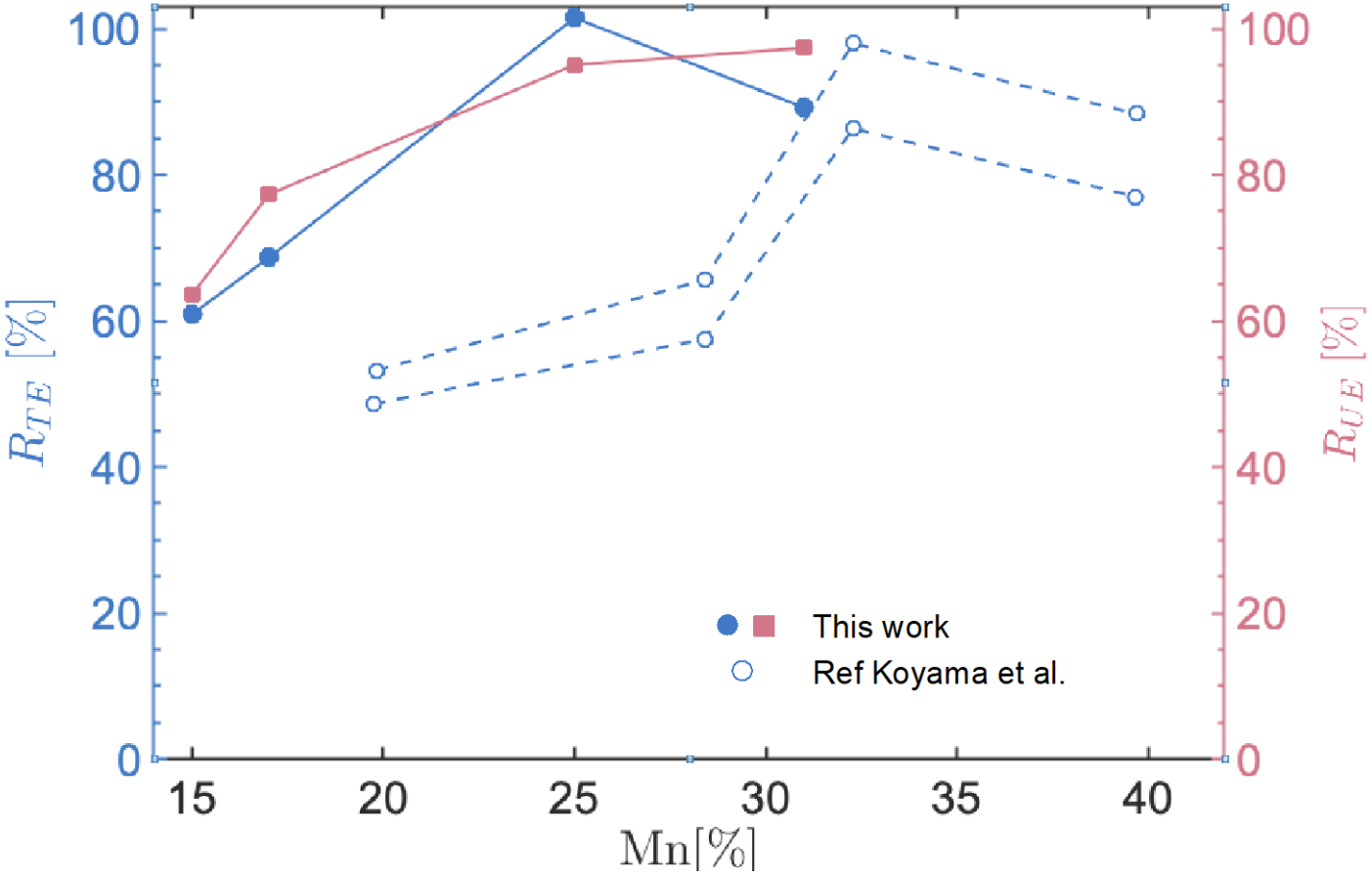

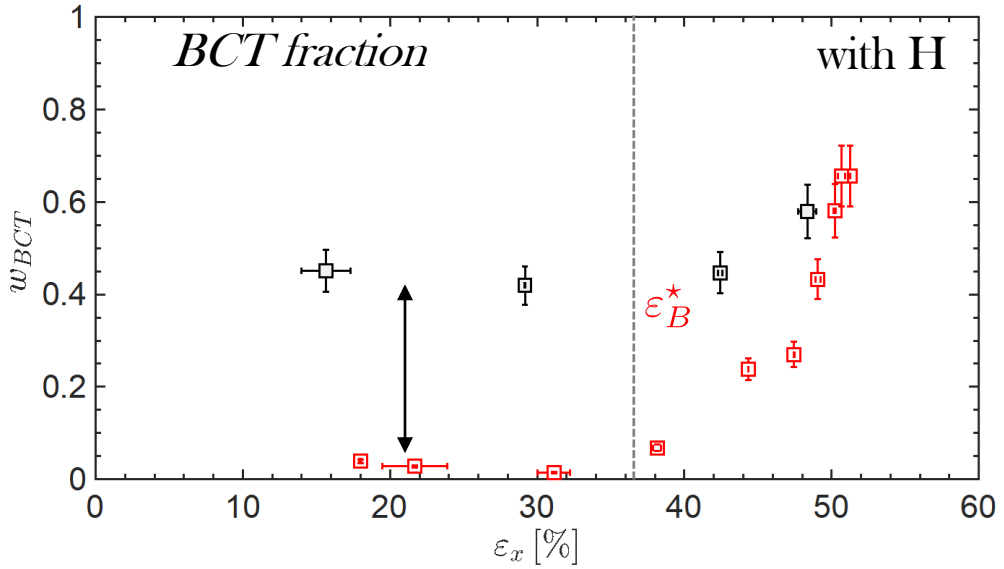

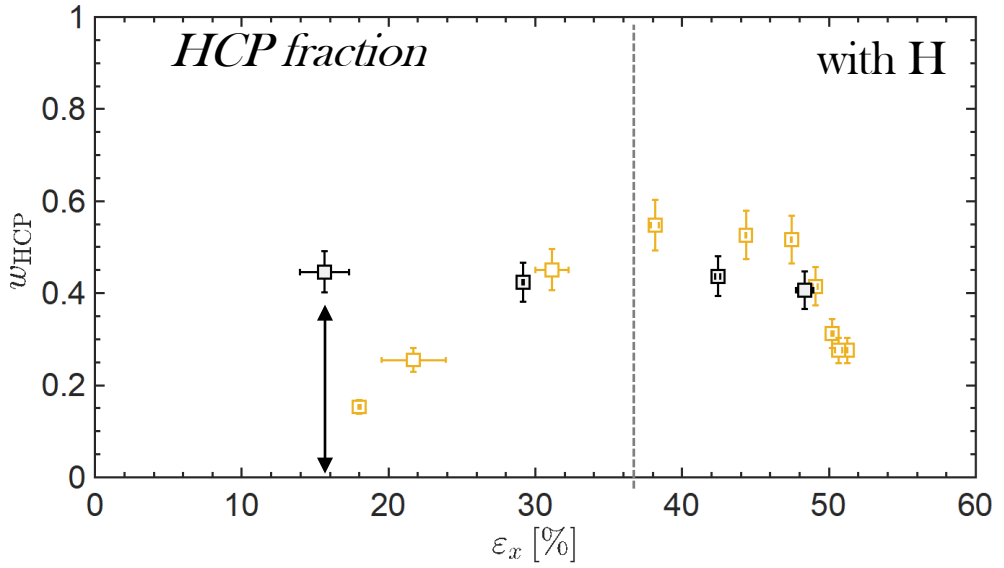

Stress Triaxiality Effects on Crack Opening in H-Charged Samples

Large-scale hybrid MD-GCMC simulations were carried to investigate the stress triaxiality effects on crack opening in a highly damaged Fe sample with H charged at a constant chemical potential.

Relatively low stress triaxiality

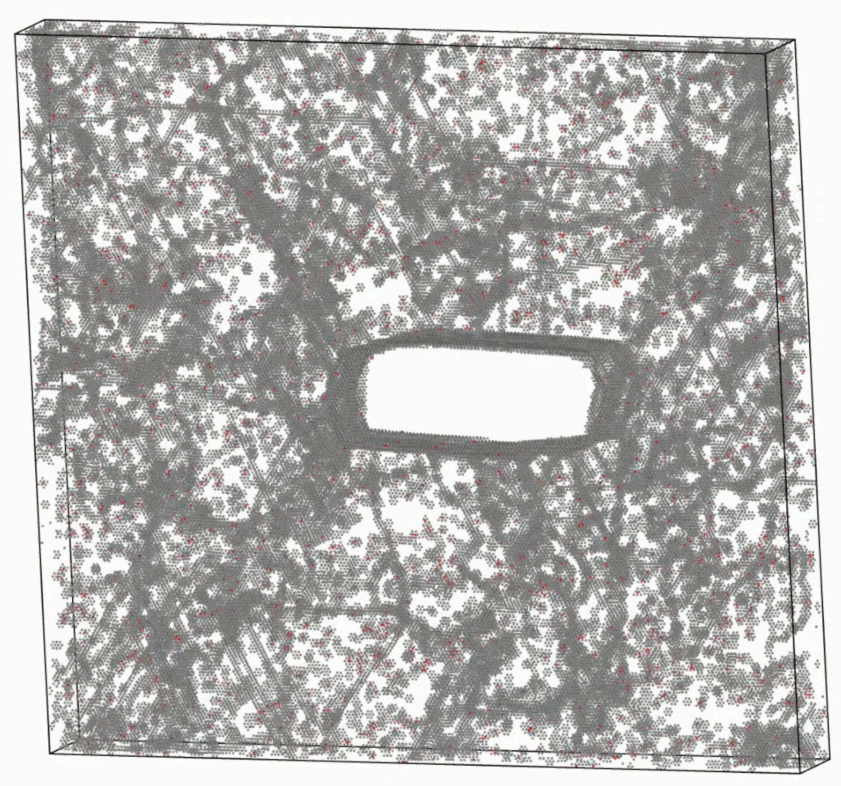

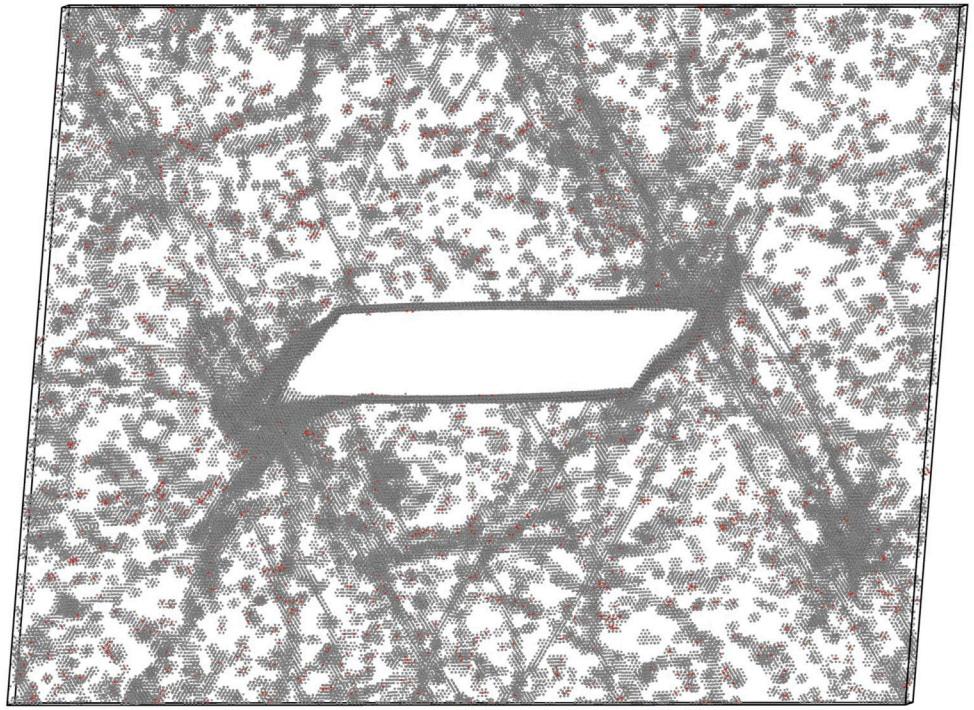

Relatively high stress triaxiality

- Real materials samples are often highly damaged and subjected to different degrees of stress triaxiality
- We created realistic samples by introducing various damages and H atoms
- Cracks under relatively low stress triaxiality condition tend to blunt up with significant plasticity at crack tip
- Cracks under relatively high stress triaxiality condition immediately open up under external load

H-Flux Induced Dislocation Motion

Our MD simulations show that a screw dislocation can move up to a few nanometers under H flux, in the absence of any external load, which is crucial to understanding experimental observations.

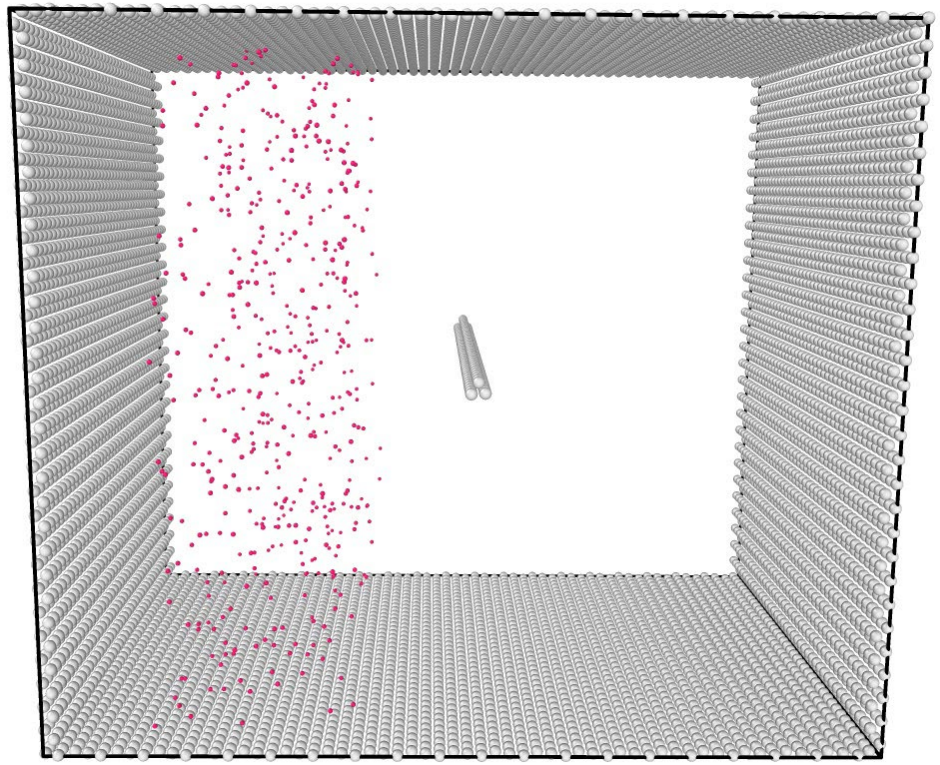

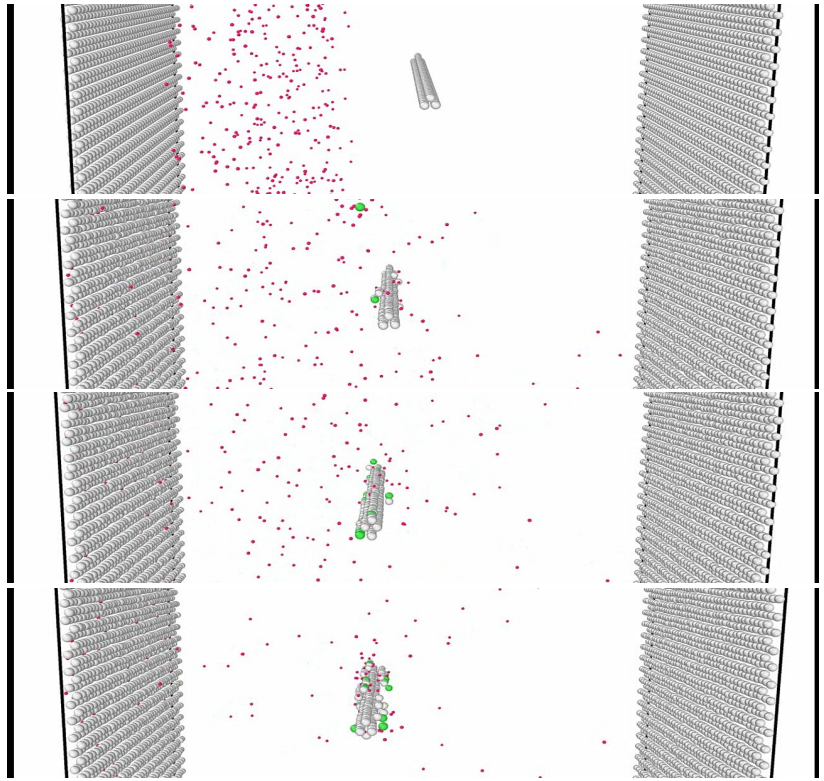

- A screw moves in the opposite direction of the H flux
- H flux provides sufficient attractive P-K force to move the dislocation
- Further interactions lead to H trapping in dislocation core, causing dislocation pinning
- MD simulations show certain limitations such as short timescale and high H flux compared to experiments

Numerical performance of the long-timescale method

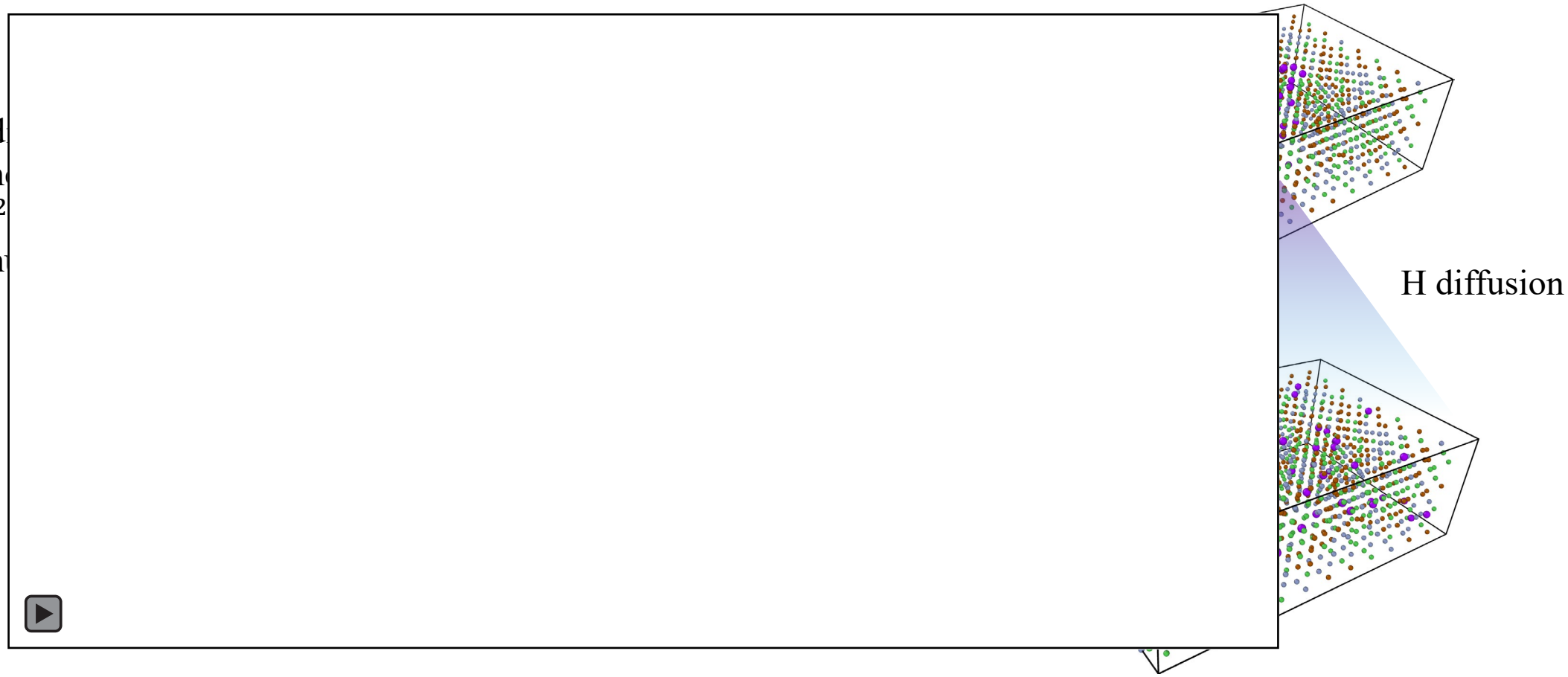

- Hydrogen diffusion in copper and equiatomic CrCoNi medium entropy alloy is simulated
- Atomic disorder in CrCoNi induces higher average transition energy barriers that decreases diffusion coefficients compared to pure metals
- Development of the method opens probabilities for long-timescale simulation of H diffusion and its interaction with dislocations and grain boundaries.

SFE Calculation methods: details

SFE calculation methods

- $\gamma_{SFE} = 2\rho\,\Delta G^{\gamma\to\varepsilon} + 2\sigma$ (Olson-Cohen [1])

  σ: γ/ε interfacial energy (treat as constant)
  ρ: {111} plane number density (constant)

  – ThermoCalc – TCFE11

  – Gibbs energy modeling for $dG^{\gamma\to\varepsilon}$

- Empirical SFE formula [2]

$$\gamma^{300}\,(\mathrm{mJ/m^2}) = \gamma^0 + 1.59\mathrm{Ni} - 1.34\mathrm{Mn} + 0.06\mathrm{Mn}^2 - 1.75\mathrm{Cr} + 0.01\mathrm{Cr}^2 + 15.12\,\mathrm{Mo} - 5.59\mathrm{Si} - 60.69\,(\mathrm{C}+1.2\mathrm{N})^{0.5} + 26.27\,(\mathrm{C}+1.2\mathrm{N})(\mathrm{Cr}+\mathrm{Mn}+\mathrm{Mo})^{0.5} + 0.61\,[\mathrm{Ni}(\mathrm{Cr}+\mathrm{Mn})]^{0.5}$$

(where γ^{300} is the value of *SFE* at room temperature and γ^0 is the value of *SFE* of pure austenitic iron at room temperature.)

Gibbs energy modeling

$$\Delta G^{\gamma\to\varepsilon} = \Delta G^{\gamma\to\varepsilon}_{mag} + \Delta G^{\gamma\to\varepsilon}_{chem}$$

$$G^{\phi}_{chem} = \sum x_i G^{\phi}_i + \sum x_i x_j \Omega^{\phi}_{i,j}$$

$$G^{\phi}_{mag} = RT\ln(\beta^{\phi}+1)\,f(\tau^{\phi})$$

x_i : atomic fraction

G^{ϕ}_i: molar Gibbs energy of element *i* of phase ϕ

$\Omega^{\phi}_{i,j}$: molar excess Gibbs energy of element *i, j* of phase ϕ

β^{ϕ}: mean magnetic moment of phase ϕ

$\tau^{\phi} = \frac{T}{T^{\phi}_{Neel}}$, T^{ϕ}_{Neel}: Neel temperature of phase ϕ

$$\mathrm{f}_{Xiong}(\tau) = \begin{cases} 0, \tau < 0 \\ 1 - \frac{1}{D} * \left[\frac{0.38438376}{t*p} + 0.63570895 * \left(\frac{1}{p} - 1\right) * \left(\frac{t^3}{6} + \frac{t^9}{135} + \frac{t^{15}}{600} + \frac{t^{21}}{1617}\right)\right], 0 < \tau < 1 \\ -\frac{1}{D} * \left(\frac{t^{-7}}{21} + \frac{t^{-21}}{630} + \frac{t^{-35}}{2975} + \frac{t^{-49}}{8232}\right), \tau > 1 \end{cases} \quad [3]$$

[1] Olson, Gregory Bruce, and Morris Cohen. "A general mechanism of martensitic nucleation: Part I. General concepts and the FCC→ HCP transformation." Metallurgical Transactions A 7.12 (1976): 1897-1904.
[2] Dai, Q. X., et al. "Structural parameters of the martensite transformation for austenitic steels." Materials characterization 49.4 (2002): 367-371
[3] Xiong, Wei, et al. "An improved magnetic model for thermodynamic modeling." Calphad 39 (2012): 11-20.